Elucidating real-world vehicle emission factors from mobile measurements over a large metropolitan region: a focus on isocyanic acid, hydrogen cyanide, and black carbon

Sumi N. Wren, John Liggio, Yuemei Han, Katherine Hayden, Gang Lu, Cris M. Mihele, Richard L. Mittermeier, Craig Stroud, Jeremy J. B. Wentzell, Jeffrey R. Brook

Air Quality Process Research Section, Air Quality Research Division, Environment and Climate Change Canada, 4905 Dufferin St., Toronto, ON, M3H 5T4

Corresponding Authors: Sumi N. Wren (sumi.wren@gmail.com), Jeffrey R. Brook (jeff.brook@canada.ca)

1 **Abstract**

2   A mobile laboratory equipped with state-of-the-art gaseous and particulate instrumentation
3 was deployed across the Greater Toronto Area during two seasons. A high-resolution time-of-flight
4 mass spectrometer (HR-TOF-CIMS) measured isocyanic acid (HNCO) and hydrogen cyanide (HCN),
5 and a high-sensitivity laser-induced incandescence (HS-LII) instrument measured black carbon
6 (BC). Results indicate that on-road vehicles are a clear source of HNCO and HCN, and that their
7 impact is more pronounced in the winter, when influences from biomass burning and secondary
8 photochemistry are weakest. Plume-based and time-based algorithms were developed to calculate
9 fleet-average vehicle emission factors (EF); the algorithms were found to yield comparable results,
10 depending on the pollutant identity. With respect to literature EFs for benzene, toluene, C2 benzene
11 (sum of m,p,o-xylenes and ethylbenzene), nitrogen oxides, particle number concentration (PN), and
12 black carbon, the calculated EFs were characteristic of a relatively clean vehicle fleet dominated by
13 light-duty vehicles. Our fleet-average EF for BC (median: 25 mg kg_{fuel}^{-1}, interquartile range: 10 – 76
14 mg kg_{fuel}^{-1}) suggests that overall vehicular emissions of BC have decreased over time. However, the
15 distribution of EFs indicates that a small proportion of high-emitters continue to contribute
16 disproportionately to total BC emissions. We report the first fleet-average EF for HNCO (median:
17 2.3 mg kg_{fuel}^{-1}, interquartile range: 1.4 – 4.2 mg kg_{fuel}^{-1}) and HCN (median: 0.52 mg kg_{fuel}^{-1},
18 interquartile range: 0.32 – 0.88 mg kg_{fuel}^{-1}). The distribution of the estimated EFs provides insight
19 into the 'real-world' variability of HNCO and HCN emissions, and constrains the wide range of
20 literature EFs obtained from prior dynamometer studies. The impact of vehicle emissions on urban
21 HNCO levels can be expected to be further enhanced if secondary HNCO formation from vehicle
22 exhaust is considered.

1. Introduction

In urban areas, traffic-related air pollution (TRAP) is associated with adverse impacts on human health, air quality, climate change, and the environment (Pope and Dockery, 2006;Grahame et al., 2014;HEI Panel, 2010). Studies of TRAP, from both the emission and exposure perspective, have often focused on criteria air pollutants such as nitrogen oxides (NO_x), carbon monoxide (CO) and particulate matter (PM) (Jerrett et al., 2009;Beckerman et al., 2008). However, it is not established to what extent these species are solely responsible for negative outcomes associated with TRAP, or to what degree they act in tandem with, or as proxies for, other compounds in the pollutant mixture (Brook et al., 2007;Mauderly and Samet, 2009;Dominici et al., 2010). That is, NO_x could be an indicator for other pollutants originating from vehicular combustion, including volatile organic compounds and particulate species (Brook et al., 2007). For that reason, it is imperative that other components of TRAP are characterized, including the near-road exposures and vehicle emission factors of air toxics. In the current study we focus on vehicle emissions of black carbon (BC), isocyanic acid (HNCO), and hydrogen cyanide (HCN).

Although particulate mass is often used as an indicator for health risks associated with combustion, it has been suggested that black carbon may be a more effective metric (Janssen et al., 2011;Grahame et al., 2014). Black carbon particles pose a significant health risk due to their chemical stability, large surface area, and small mode diameter, with the smallest (i.e., 'ultrafine') BC particles able to penetrate the lung lining and enter the blood stream (Highwood and Kinnersley, 2006). However, it is not established whether it is the compounds associated with BC (such as particle bound polycyclic aromatic hydrocarbons) or the BC itself that are responsible for negative effects (Janssen et al., 2011). The dominant sources of BC are combustion-related and include open biomass burning (BB) and residential, industrial, and transportation-related fossil-fuel burning. Anthropogenic BC emissions have been closely linked to vehicle emissions, particularly those associated with heavy-duty diesel vehicles (HDDV) (Bahadur et al., 2011;Ban-Weiss et al., 2008). Although, BC emissions from light-duty gasoline vehicles (LDGV) have been considered to be quite low by comparison, their exact magnitude is not well constrained, with recent studies suggesting that they may both be underestimated (Liggio et al., 2012;Krecl et al., 2017) and overestimated (Wang et al., 2016). Furthermore, improvements in emissions control technologies have seen HDDV BC emissions decrease significantly (Dallmann et al., 2012;Krecl et al., 2017). As a result, the relative importance of gasoline versus diesel engines as sources of BC is not well established, leading to uncertainties in present-day on-road inventories (Liggio et al., 2012;Krecl et al., 2017). Given the rapid pace of change of fuel injection and emission control technologies, establishing current, fleet-average BC emission factors (EF) is important for evaluating bottom-up inventories, which are necessary from both a health/air quality and climate perspective (Bond et al., 2013).

Only recently has it been suggested that HNCO (Wentzell et al., 2013;Brady et al., 2014;Link et al., 2016;Suarez-Bertoa and Astorga, 2016;Jathar et al., 2017) and HCN (Crounse et al., 2009;Moussa et al., 2016;Harvey et al., 1983) can be emitted by on- and off-road vehicles. Isocyanic acid is a highly toxic gaseous acid which dissociates at physiological pH to form cyanate anions (NCO−) which in turn participate in damaging carbamylation reactions, thereby leading to adverse

health outcomes such as cataracts, atherosclerosis, rheumatoid arthritis, cardiovascular disease, and renal failure (Roberts et al., 2011 and references therein). Roberts et al. (2011) used the physical properties of HNCO to estimate that ambient mixing ratios as low as 1 ppbv could be harmful to humans (Wang et al., 2007). Similar to HNCO, hydrogen cyanide is a highly toxic gas with known negative effects on human health due to its interference in aerobic metabolism (Logue et al., 2010;Barillo, 2009; U.S. EPA, 2010).

Historically, biomass burning was considered to be the dominant global source of both HNCO (Veres et al., 2010;Roberts et al., 2011;Young et al., 2012) and HCN (Li et al., 2000;Li et al., 2003;Li et al., 2009;Shim et al., 2007). Global HCN (Li et al., 2003) and HNCO (Young et al., 2012) models have hitherto considered vehicle sources of these compounds to be negligible. As such, past measurements of these species have focussed on regions heavily influenced by biomass burning, or in the case of HCN, on the upper troposphere or total tropospheric column. Although the advent of chemical ionization mass spectrometers has allowed for real-time measurements of atmospherically relevant concentrations of these species (Roberts et al., 2011;Veres et al., 2008;Woodward-Massey et al., 2014;Le Breton et al., 2013;Knighton et al., 2009), there remain relatively few measurements of ambient HNCO (Roberts et al., 2011;Roberts et al., 2014;Wentzell et al., 2013;Zhao et al., 2014;Woodward-Massey et al., 2014;Sarkar et al., 2016;Chandra and Sinha, 2016; Kumar et al., 2018). Measurements of ground-level HCN in both rural and urban environments with minimal BB influence are more limited (Ambrose et al., 2010). However, given the recent studies suggesting that HCN and HNCO emissions from vehicles could be significant, especially at a local scale, a better understanding of on-road emissions of these species is necessary. Moreover, ambient measurements are suggestive of a secondary source of HNCO (Roberts et al., 2011;Wentzell et al., 2013;Roberts et al., 2014;Zhao et al., 2014;Sarkar et al., 2016; Kumar et al., 2018) – formed photochemically by the photooxidation of precursors such as alkyl amines and amides (Borduas et al., 2013;Borduas et al., 2015;Sarkar et al., 2016). Recent studies (Jathar et al., 2017;Link et al., 2016) show that diesel engine exhaust itself contains precursors leading to enhanced photochemical production of HNCO, even further underscoring the need to quantify vehicular emissions of HNCO in dense, urban environments.

Existing literature values for HNCO and HCN emission factors have been exclusively obtained from chassis or engine dynamometer studies on a limited number of engines/vehicles. While the strength of dynamometer studies is control over factors such as vehicle age, fuel composition, type of after-treatment technologies, temperature, and driving mode, they have limitations with respect to yielding representative emission factors, for the precise reason that mobile emissions have been shown to be sensitive to such factors (Franco et al., 2013). It is important that the accuracy of emission inventories derived from dynamometer results are verified against in-use vehicle emissions (Parrish, 2006), since emission inventories are often used to constrain regional budgets and exposure estimates for traffic-related air pollutants. This is particularly relevant for HNCO and HCN, where there are large discrepancies in reported emission factors. Although real-world EF measurements can suffer from their own shortcomings (namely lower precision and repeatability), they are essential in identifying gaps and providing insight into actual emission behaviour of on-road vehicles (Franco et al., 2013).

1   In the present study, we deploy a mobile laboratory over a large metropolitan region in two
2   seasons, with the goal of characterizing near-road exposure and fleet-average emission factors for
3   black carbon, HNCO, and HCN. These species are discussed alongside benzene, a regulated traffic
4   pollutant of interest due to its carcinogenic nature, and whose behaviour has been more thoroughly
5   characterized. The focus in this paper is on the development of plume-based and time-based
6   methodologies to calculate fuel-based vehicle emission factors. We assess their performance
7   against each other and in comparison to available literature EFs for a wide range of pollutants:
8   benzene, toluene, C2 benzenes (sum of m,p,o-xylenes and ethylbenzene), NO_x (=NO + NO_2), particle
9   number concentration (PN), and black carbon. We report, to our knowledge, the first real-world,
10   fleet-average HNCO and HCN vehicle emission factors and use them to help assess dynamometer
11   results relative to real-world conditions. Finally, the estimated fleet-average emission factors are
12   scaled-up to determine the relative importance of vehicle emissions of HNCO and HCN.

13   **2.   Materials and Methods**
14   **2.1. Mobile laboratory measurements – CRUISER**
15   **2.1.1.   Overview of mobile measurements**

16   Air quality and meteorological measurements were made from Environment and Climate
17   Change Canada's mobile laboratory: Canadian Regional and Urban Investigation System for
18   Environmental Research (CRUISER) (Levy et al., 2014). CRUISER was deployed during two seasons
19   over the Greater Toronto Area (GTA), a metropolitan area encompassing the city of Toronto and
20   four regional municipalities with a population of over 6 million. The Summer Campaign took place
21   over 9 days in July, 2015 (July 15, 16, 17, 20, 21, 22, 23, 27, 28) as part of the Environment Canada
22   Pan and Parapan American Science Showcase (ECPASS) (Joe et al., 2018). The Winter Campaign
23   took place over 8 days in January, 2016 (January 11, 13, 14, 15, 18, 19, 20, 21) as part of a health
24   exposure mapping study. Driving took place on weekdays only, with the majority of measurements
25   occurring between 09:00 and 17:00 local time. Driving routes were chosen to pass along highways,
26   major roadways, and local streets, and to visit residential, commercial, and industrial areas; the
27   driving routes for the Summer and Winter Campaign are shown in Supplement Fig. S1. In 2016 the
28   Ontario vehicle fleet was composed of approx. 97% light-duty (LD) vehicles (vehicles < 4500 kg and
29   motorcycles/mopeds) and 4% heavy-duty (HD) vehicles (for this paper, the HD category includes
30   both medium-duty vehicles 4500 – 14 999 kg and heavy-duty trucks > 15 000 kg, and buses)
31   (Statistics Canada); the composition of the GTA vehicle fleet is assumed to be similar.

32   Several gas phase and particle phase instruments were housed on-board CRUISER as listed
33   in Table 1. Carbon dioxide (CO_2) was measured with 2 s time resolution by cavity-enhanced laser
34   absorption spectroscopy (PICARRO). All gas phase instruments sampled from a common inlet with
35   the exception of the high-resolution time-of-flight chemical ionization mass spectrometer (HR-TOF-
36   CIMS) which sampled off a dedicated inlet located on the roof of CRUISER towards the rear right-
37   side. The common gas phase inlet was located 3.6 m a.g.l. and oriented near the front left side.
38   Ambient air was sampled through a 2 m long PFA tube with 0.61 cm ID followed by a 30 cm long
39   PFA tube with 0.52 cm ID at a rate of 13.6 slpm (residence time ~ 0.25 s); inlet lines for various
40   instruments were connected downstream of this common inlet. All particle phase instruments
41   sampled off a common stainless steel inlet located adjacent to the gas phase inlet. During the Winter

Campaign, CO_2 was sampled from the same inlet as the HR-TOF-CIMS. Relative wind speed and wind direction was measured using an ultrasonic anemometer located on the roof at the front of CRUISER. Periods of potential self-sampling were identified and removed using an algorithm which is described in the Supplement. Briefly, the self-sampling algorithm identified periods of 'potential' exhaust based on CRUISER speed, relative wind speed, and wind direction (towards inlet) and periods of 'suspected' exhaust within these windows, based on the presence of exhaust tracers (BC, NO, fine particle counts). Periods of 'suspected' exhaust were removed from the data.

2.1.2. Proton-transfer reaction time-of-flight mass spectrometry (PTR-TOF-MS)

Volatile organic compounds (VOC) were measured using a proton transfer reaction time-of-flight mass spectrometer (PTR-TOF-8000, Ionicon Analytik). The operating principles of the PTR-TOF-MS instrument have been described elsewhere (Jordan et al., 2009;Li et al., 2017); further details can be found in the Supplement. Briefly, the PTR-TOF-MS was operated with an E/N value of 140 Td. Air for analysis by the PTR-TOF-MS was sampled off the common gas phase inlet via a 2 m long PFA tube with 0.52 cm ID at a rate of 4.4 sLpm and the instrument sampled part of this flow (100 sccm) through a 120 cm insulated PEEK capillary with 0.08 cm ID heated to 70°C. Mass spectra were acquired with a time resolution of 1 s and a resulting mass resolution of approx. 4000 m/Δm. The response of the PTR-TOF-MS to specific VOCs was determined using a home-built zero/calibration unit and a custom VOC gas standard (Ionicon). The 2σ detection limits differed slightly for the Summer and Winter Campaigns and were calculated respectively to be 110 pptv and 155 pptv for benzene, 125 pptv and 240 pptv for toluene, and 110 pptv and 160 pptv for C8 benzenes. The sensitivities and detection limits are also listed in Table S1.

2.1.3. High resolution time-of-flight chemical ionization mass spectrometer (HR-TOF-CIMS)

HNCO and HCN were measured using a high-resolution time-of-flight chemical ionization mass spectrometer (HR-TOF-CIMS, Aerodyne Research, Inc.). The design, operation and mobile deployment of the HR-TOF-CIMS has been previously described (Veres et al., 2008;Roberts et al., 2011;Wentzell et al., 2013;Liggio et al., 2017a). Additional details can be found in the Supplement. Briefly, the HR-TOF-CIMS is a differentially pumped time-of-flight mass spectrometer configured to use iodide ion as the reagent ion (Woodward-Massey et al., 2014;Le Breton et al., 2013). Air for analysis was drawn at ~22 sLpm through a 3 m long heated (50 °C) inlet (0.58 cm ID). The CIMS subsampled from this flow into the molecule reaction (IMR) region via a critical orifice at 1.7 sLpm. Mass spectra were acquired with a time resolution of 1 s and a resulting mass resolution of approx. 5000 m/Δm. Calibrations of HNCO were conducted by thermally decomposing cyanuric acid at 250 °C to HNCO (Roberts et al., 2010) with the permeation rate quantified via Fourier Transform Infrared Spectroscopy (FTIR; Thermo-Fisher Inc.). Calibrations of HCN were performed by diluting a HCN gas standard (Air Liquide, ppmv in N_2) in zero air. Humidity dependant response factors for both species were derived by diluting the calibration gas flows with humidified air to a final RH ranging from ~9% to 90%, resulting in sensitivities of 0.086 ncps/pptv and 0.1 ncps/pptv for HCN and HNCO respectively. The 2σ detection limits for HNCO and HCN were estimated to be 7 pptv each for both the Summer and Winter Campaigns.

2.1.4. High-sensitivity laser-induced incandescence (HS-LII) for Black Carbon

Black carbon measurements were made with a high-sensitivity laser-induced incandescence (HS-LII) instrument (Atrium Technologies Inc., CA, USA) developed in collaboration with the National Research Council Canada (NRC). The particular instrument on CRUISER is a research-grade prototype capable of ultra-low BC measurements at 1 s resolution. Here, black carbon is operationally defined by its high thermal stability (Petzold et al., 2013). The principle of operation of this instrument, as well as its use during ambient studies, has been described elsewhere (Snelling et al., 2005;Chan et al., 2011;Liggio et al., 2012). Briefly, ambient particles within a set volume are rapidly heated by a pulsed laser beam (1064 nm; 7 ns FWHM, 200 mJ/pulse) to just below the soot sublimation temperature (∼4000 K). The absolute incandescence and temperature of the BC particles are measured by collection optics and photomultipliers. After appropriate calibration and analysis, these two parameters are used to determine the soot volume fraction, which is converted to a BC mass concentration with knowledge of the particle material density (ρ) and the absorption function (E_m), both of which are well-established for BC (Coderre et al., 2011;Choi et al., 1994;Wu et al., 1997). An advantage of this technique is that it determines ensemble properties for all particles within the sample volume and so does not suffer from a particle size limitation; previous studies have shown that the HS-LII can detect laboratory generated particles < 7 nm in diameter (Stirn et al., 2009). As a result, a previous study found that BC measurements by a single-particle soot photometer (SP2), which is only sensitive to particles with a diameter > 70 nm, are biased low relative to the HS-LII (Liggio et al., 2012). Furthermore, it has been shown that the HS-LII is significantly less-influenced by the presence of non-refractory mass compared to other BC measurements methods such as photoacoustic spectrometers (Chan et al., 2011).The HS-LII was only in operation for the Summer Campaign.

2.2. Calculating fleet-average emission factors from a mobile platform

Mobile measurements (Jiang et al., 2005;Canagaratna et al., 2004;Zavala et al., 2006;Zavala et al., 2009;Park et al., 2011;Liggio et al., 2012;Hudda et al., 2013;Jimenez et al., 2000) of individual tailpipe emissions (i.e. plumes) have proven to be an effective approach for determining fleet emission factors, with the advantage of covering a large geographical region, while measuring emissions in real-time over a range of driving modes. Hence they are able to evaluate the applicability of EF measurements made at a fixed location to the entire region, providing insight into the degree of emissions variability and identifying the presence of high-emitting vehicles.

Plume-based emissions measurements can be made in two ways: a targeted approach in which individual vehicles are 'chased' (Canagaratna et al., 2004;Zavala et al., 2009;Zimmerman et al., 2016), or a 'catch-all' approach in which all intercepted plumes are treated as potential exhaust plumes (Jimenez et al., 2000;Jiang et al., 2005;Zavala et al., 2009;Hudda et al., 2013;Wang et al., 2015). The advantage of the 'catch-all' approach is that a large number of plumes can be encountered, leading to improved statistics for characterizing the fleet on the road in the domain of study (Zavala et al., 2009;Wang et al., 2015). Alternatively, emission factors from mobile measurements can be determined using a time-based or road segment-based approach in which pollutant concentrations above background are evaluated at fixed time or distance intervals (Hudda

1 et al., 2013;Westerdahl et al., 2009;Zavala et al., 2006;Zavala et al., 2009). Here, we calculate fleet
2 emission factors using both a 'catch-all' mobile plume-based approach and a time-based approach.

2.2.1. Definition of background (BKG) and local (LOCAL) concentrations

4   Pollutant and CO_2 time series were averaged to 2 s and then further smoothed using a 3
5 point boxcar (5 s). The background (BKG) was subsequently defined as the rolling 2nd percentile
6 over a 90 point (180 s) window, with additional boxcar smoothing over the same window. Similar
7 approaches for estimating background concentrations from mobile monitoring studies have been
8 employed by others (Jiang et al., 2005;Jimenez et al., 2000;Hudda et al., 2013;Park et al.,
9 2011;Bukowiecki et al., 2002;Larson et al., 2017). Since the background is calculated over a 3 min
10 window, corresponding to approximately 2 km of CRUISER travel, it is assumed to be
11 representative of a neighbourhood scale background (Larson et al., 2017). The "on-road"' or LOCAL
12 concentrations are defined as the background-corrected (i.e., above-background) mixing ratios.
13 Figure S2 shows sample time series for the Summer (CO_2, benzene, BC, HNCO, HCN) and Winter
14 Campaigns (CO_2, benzene, HNCO, HCN) and demonstrates that the LOCAL pollutant plumes
15 frequently co-varied with increases in CO_2, suggesting a combustion (i.e. vehicular) source.

2.2.2. Plume-based emission factor determination

17   An emission factor algorithm was written using Igor Pro (Wavemetrics Inc.) to identify CO_2
18 plumes based on the first and second derivatives of the CO_2 time series, similar to the approach of
19 Wang et al. (2015). The details of the algorithm can be found in the Supplement. Briefly, the first
20 derivative of the CO_2 time series was used to identify peak boundaries and locations (peak
21 maxima). Two types of plumes were identified: single peak plumes (SPP) and multi-peak plumes
22 (MPP). Multi-peak plumes contain one or more CO_2 peaks (and include the SPP set). Plumes less
23 than 10 s in duration or with an average background-corrected CO_2 response of < 5 ppmv s^{-1} over
24 the integration period were rejected as erroneous or uncaptured (Wang et al., 2015). Emission
25 factors (EF) expressed as mg kg-fuel^{-1} for a given pollutant X and plume i were calculated using a
26 carbon mass balance approach:

$$EF_{X,i} = \frac{[X]}{[CO_2]} \times \frac{MW_X}{F_C \cdot MW_C} \times C_{fuel} \times 10^3 \quad [1]$$

28 Where [X] and [CO_2] are the integrated amounts of LOCAL (background-corrected) X and CO_2 over
29 the boundaries of plume *i* in units of ppmv and ppbv respectively, MW_X and MW_C are the molecular
30 weights of pollutant X and carbon in g mol^{-1}, F_C Is the molar ratio of carbon in CO_2, C_{fuel} is the carbon
31 mass fraction in the fuel in kg C kg$_{fuel}$$^{-1}$, and 10^3 is the necessary unit conversion factor. A value of
32 $C_{fuel} = 0.86$ was used here, which is the average of the C_{fuel} for gasoline (0.85) and diesel (0.87)
33 (Wang et al., 2015). Strictly, the denominator in Eq. 1 should contain the sum of all emitted carbon
34 species (CO_2, CO, total hydrocarbons); however, emissions of CO_2 have been shown to account for $>$
35 90% of fuel consumption (Jathar et al., 2017;Yli-Tuomi et al., 2005). Plumes associated with the
36 highest EFs were visually inspected and in some instances were deemed to have been 'erroneously
37 captured' based on poor correlation between the pollutant and CO_2 time series; these plumes were
38 removed from the final dataset. Further details regarding the background calculation and their

1 influence on calculated EFs, and the peak removal processes can be found in the Supplement
2 (Section 1.5).

3   Emission factors for benzene, toluene, C2 benzenes, NO, NO_2, NO_x, PN, and BC were obtained
4 during the Summer Campaign. EFs for HCN and HNCO were obtained during the Winter Campaign,
5 when the PICARRO measuring CO_2 shared the same inlet as the HR-TOF-CIMS. Statistics on the
6 number of plumes, plume duration, and number of peaks per plume can be found in Table S2 and
7 S3 at various stages of analysis for the Summer and Winter Campaigns. We note that for NO,
8 reactions with ozone can result in a low bias for NO EFs. In this study we expect the time from
9 emission to be on the order of minutes, although exact emission times are not known. As such it is
10 likely that the EF for NO here represent lower limits to the true NO EFs.

11   **2.2.3.   Time-based emission factor determination**

12   Emission factors were also calculated using the time-based approach, which considers the
13 entire data set, in contrast to the plume-based approach which only considers periods of elevated
14 CO_2 as defined by peaks (Westerdahl et al., 2009). The LOCAL (background-corrected) CO_2 and
15 pollutant mixing ratios were integrated in consecutive intervals of 30, 60, 90, and 120 s and fuel-
16 based emission factors were calculated according to Eq. 1.

17   This approach assumes that LOCAL mixing ratios are solely due to vehicle emissions (in reality,
18 they may also contain point sources or other types of emissions, including those not associated with
19 combustion). The purpose of this calculation was two-fold. First, we were interested in determining
20 whether this computationally simple approach could yield realistic fleet-average emission factors
21 comparable to those obtained using the plume-based approach. Second, we were interested in
22 determining EFs for pollutants not sharing a common inlet with CO_2 (i.e., for benzene/BC during the
23 winter, and HNCO/HCN during the summer), which would allow for a seasonal comparison. Here,
24 the assumption is that when integrating over a sufficiently long interval of time, the majority of
25 vehicle plumes are captured by both inlets (i.e., both the CO_2 and pollutant X are detected), and that
26 meteorology/turbulence affects the dilution of the pollutant and CO_2 equally.

27 **3. Results and Discussion**
28 **3.1. Overview of mobile pollutant measurements**

29   Ambient pollutant concentration statistics for the Summer Campaign (benzene, toluene, C2
30 benzenes, NO_2, NO, CO_2, PN, BC, HNCO, HCN) and Winter Campaign (benzene, HNCO, HCN, and CO_2)
31 are shown in Table 1. The BC concentrations reported in this study are comparable to the range
32 (0.10 – 1.7 µg m^{-3}) previously reported for Toronto (Knox et al., 2009;Chan et al., 2011).

33   The ambient HNCO concentrations measured during this study are similar in magnitude to
34 those measured by others (Roberts et al., 2011;Roberts et al., 2014;Woodward-Massey et al.,
35 2014;Zhao et al., 2014;Wentzell et al., 2013) for urban locations with minimal BB influence, which
36 range from *ca.* 10 – 85 pptv. However, Chandra and Sinha (2016) report annual HNCO mixing ratios
37 of 0.94 ppbv for a suburban site in the Indo-Gangetic Plain that is strongly influenced by crop-
38 residue fires; a much higher average summertime HNCO concentration of 1.7 ± 0.06 ppbv was
39 recently measured at the same site (Kumar et al., 2018). Our measurements for both the summer

and winter periods are slightly lower than the summertime mean mixing ratio of 85 pptv previously reported for a fixed location in Toronto (Wentzell et al., 2013). However we note that the authors found that HNCO was generally highest between the hours of 18:00 and 22:00. In the present study, the measurements are limited to the driving period, which could explain the slightly lower mean HNCO concentration. Overall, the magnitudes of the HNCO mixing ratios in both seasons (~45 pptv and ~26 pptv for the summer and winter, respectively) are much lower than the 1 ppbv harm threshold (Roberts et al., 2011; Wang et al., 2007).

The HCN mixing ratios measured in this study are two orders of magnitude lower than the mean HCN mixing ratios of 3.45 ± 3.43 ppbv (continuous sampling from a near-road location) and 1.57±0.33 ppbv (mobile measurements in heavy traffic) previously reported for Toronto (Moussa et al., 2016). Long-path FTIR measurements of HCN (1 min time resolution) were made above the busy HWY 401 in Toronto concurrent to the present study (July – Aug 2015) (You et al., 2017). Consistent with our low HCN measurements, the authors found that HCN mixing ratios only spiked above the FTIR method detection limit of 3.2 ppbv on 3 occasions (isolated 1 min data points). Although prior measurements (Moussa et al., 2016) seem exceptionally high, our measurements are also on the low end of those reported for ground level, ambient HCN in a rural region with little forest fire impact, which are on the order of a few hundred pptv (Ambrose et al., 2012). No significant long-term changes have been observed or expected for tropospheric HCN (Zhao et al., 2002) so it is unclear as to why the present measurements are so low. However, the vast majority of HCN measurements have focused on regions influenced by biomass burning and have been made aloft; measurements of HCN at ground level in urban areas are severely lacking. More measurements of HCN in urban environments are required in order to better characterize HCN concentration gradients and population exposure in regions with minimal biomass burning influence.

3.1.1. Local ("on-road") and background contributions: A seasonal comparison

Figure 1 shows histograms as a function of season for the measured ambient concentrations as well as for the background (BKG) and "on-road" (LOCAL) contributions for (a) HNCO and (b) HCN; Fig. S4 shows similar histograms for (a) benzene and (b) black carbon. Figure 2 shows the mean BKG and LOCAL contributions to the measured ambient concentration for the four pollutants, as a function of season. For both benzene and BC, the LOCAL contribution is dominant, indicating strong traffic sources for these pollutants. We observed a small seasonal dependence in ambient benzene, with overall higher concentrations in the winter than in the summer, as observed by others (Tan et al., 2014;Lough et al., 2005). Separation of the observations into the BKG and LOCAL contributions reveals that the shift is largely in the LOCAL contribution rather than the BKG contribution, consistent with an enhanced wintertime emission factor for benzene (Tan et al., 2014;Lough et al., 2005), attributed to higher cold-start emissions and changes in fuel composition. An enhancement in wintertime benzene concentrations may also be partially attributed to an increase in benzene emissions from residential wood combustion (e.g., wood stoves, fireplaces). This enhancement would manifest in the BKG contribution (which is indeed slightly higher in the winter than the summer). On a national scale, this source is significant (Canada-Wide Standard for Benzene 2010 Final Report , 2012), however, in urban areas, wood heating is the primary home

heating fuel for <0.1% of residences (Matz et al., 2015), and so it is unlikely that this source is significant within the GTA. Increases in wintertime benzene may also be attributed to a shallower boundary layer height. A seasonal comparison is not available for black carbon.

To our knowledge, our dataset represents the first seasonal comparison of ambient HNCO measurements made at the same location. Figure 2c illustrates a decrease in HNCO concentrations from the summer to the winter. Shallower boundary layer heights would be expected to lead to enhanced wintertime concentrations if HNCO emissions/sources remain constant, and yet we observe lower concentrations of HNCO in the winter. Hence the boundary layer height is a potential issue that can reduce the apparent differences between summer and winter. Further inspection of Fig. 1a and 2c reveals that the seasonal difference is largely in the BKG contribution rather than the LOCAL contribution. The lower HNCO mixing ratios in the winter could be due to a reduction in photochemical activity and/or source strength of secondary HNCO precursors (e.g., biogenic amines) (Woodward-Massey et al., 2014;Roberts et al., 2014), or due to decreased influence from biomass burning. However, the extent to which wild fires contribute to summertime HNCO concentrations is not well established and may be less significant given HNCO's moderate lifetime (as short as a few hours in clouds, but typically weeks to hundreds of years) (Borduas et al., 2016;Barth et al., 2013;Zhao et al., 2014), and the distant location of major Canadian wildfire events relative to Toronto. Although residential wood burning could also contribute to HNCO across the GTA in the winter, a recent study by Coggon et al. (2016) showed that common residential wood fuels (e.g., heartwood and sapwood) have low nitrogen content and thus lower emissions of nitrogen-containing VOCs such as HNCO and HCN. Consistent with this finding and the low incidence of residential wood burning in the GTA (Matz et al., 2015), the HNCO BKG component is low in the winter. Rather, the LOCAL component dominates the contribution to the measured HNCO in the winter, indicating the significance of on-road emissions as an HNCO source. Although lower temperatures are thought to enhance HNCO vehicle emissions (particularly cold-start emissions) (Suarez-Bertoa and Astorga, 2016), the similarity in the magnitude of the LOCAL component between seasons suggests that, overall, the primary on-road HNCO emissions remain relatively constant.

Similar to HNCO, we observe a strong seasonal dependence for HCN. The histogram in Fig. 1b shows a much broader distribution and higher mean for the summer compared to the winter (Fig. 2d). Separation of the observations into BKG and LOCAL contributions in Fig. 1b reveals a strong seasonal difference for both components, although the difference is more striking for the BKG component. As with HNCO, despite shallower boundary layer heights in the winter, the overall concentrations are observed to be lower in the winter. The same arguments regarding the potential impact of residential wood burning on wintertime HNCO emissions apply to HCN. The large increase in BKG in the summer is consistent with the wildfire season in Canada, and that biomass burning is thought to be the major source of HCN to the atmosphere. Given the relatively long lifetime of HCN (~2-5 months) (Li et al., 2003) compared to HNCO, biomass burning episodes in other parts of Canada would be expected to have a greater potential to influence background HCN in Toronto compared to HNCO. A strong seasonal pattern for HCN has previously been observed for tropospheric HCN column measurements (Zhao et al., 2002); seasonal measurements of HCN at an urban location have not been made. The bulk of the total measured HCN concentration is in the BKG component rather than the LOCAL component, especially in the summer, suggesting that in relative terms, on-road HCN sources may be less significant than other regional or global sources. This is in

1   contrast to benzene (dominant LOCAL component in both seasons) and HNCO (dominant LOCAL

2   component only in the winter). Interestingly, examination of Fig. 1b also reveals a strong seasonal

3   dependence in the LOCAL component, suggesting a possible seasonal dependence in the on-road

4   HCN emissions, as discussed below (Sect. 3.3.3).

5   **3.2. Comparison of plume-based vs time-based emission factor methodologies**

6   A discussion of trends within the plume-based and time-based emission factors, as well as a

7   thorough comparison of the two methodologies can be found in the Supplement for all species

8   (Tables S6 and S7). Median EFs calculated using both the plume-based SPP approach and time-

9   based approach (120 s interval) are also compared graphically in Fig. 3 for benzene, HNCO, and

10   HCN. We find the time-based approach yields much higher (> 80%) median EFs for black carbon

11   and NO than the plume-based approach. As discussed in the Supplement, the exact reason for the

12   discrepancy is not known. However we note that both BC and NO are strongly associated with

13   HDDV vehicles and thus exhibit highly skewed EF distributions, and that the time-based approach

14   does not appear to adequately capture the small EF end of these distributions (Fig. S6). In contrast,

15   we find that the two approaches yield median EFs within 25% for species associated with LDGV

16   emissions (benzene, toluene, C2 benzenes, NO_2, PN, HNCO, and HCN) (see Fig. 3, Table S6, and Table

17   S7). The ability of the time-based methodology to capture similar EF trends (Fig. S7) and

18   magnitudes as the plume-based approach for the majority of pollutants shows that this

19   computationally simple analysis can provide basic insight regarding fleet-average emissions,

20   although more work is required to fully understand the conditions/pollutants which are best suited

21   to this approach. In the current study, the advantage of the time-based methodology is its ability to

22   reveal seasonal trends in emission factors, which are reflections of the changing LOCAL ("on-road")

23   contributions. However, this method could potentially have useful applications for monitoring long-

24   terms trends in vehicle emissions using near-road surveillance data or data from instruments with

25   insufficient time resolution for a plume-based analysis. Since the LOCAL component used in the

26   analysis may also include near-road or non-mobile sources, the EFs calculated using this method

27   likely represent an upper bound.

28   Ultimately, periods of vehicle exhaust are defined with the highest confidence using the plume-

29   based SPP approach and so we expect that this methodology yields the most accurate EFs. Because

30   individual plumes are more likely to be associated with specific vehicles using this methodology, it

31   also provides insight as to the variability of vehicle EFs and the presence of high-emitters within the

32   fleet. Since the mean and standard deviation are sensitive to distortion by the presence of high-

33   emitting vehicles in our modest sample sizes, we, and others (Westerdahl et al., 2009), suggest that

34   the median and interquartile range (IQR) are more representative metrics for comparison with

35   literature emission factors and for estimating inventories. Therefore all further discussion focuses

36   on median EFs obtained using the plume-based SPP methodology unless stated otherwise. The

37   distribution histograms of plume-based EFs are shown in Fig. 4 for benzene, BC, HNCO, and HCN

38   and in Fig. S5 for others traffic pollutants (toluene, C2 benzenes, NO, NO_2, NO_x, and PN).

39   **3.3. Plume-based fleet emission factors for common traffic pollutants**

Our results are now compared to literature EFs for common traffic pollutants (benzene, toluene, C2 benzenes, NO_x, PN, BC). In the subsequent sections, the fleet-average EFs estimated for black carbon, HNCO, and HCN are discussed in further detail.

Plume-based median, mean, and interquartile range SPP EFs for a number of traffic pollutants are listed in Table 2, along with literature EFs obtained from tunnel, mobile, near-road or remote-sensing studies. The median/mean plume-based EFs calculated here are consistent with, but generally fall on the lower-end of, the EFs reported in the literature. The lower EFs obtained here may be a result of the study location: fleet-average EFs are highly sensitive to the make-up of the vehicle fleet (i.e., vehicle age, proportion of gasoline vs diesel vehicles, after-treatment technologies in use), which is in turn location dependent (Kristensson et al., 2004;Zavala et al., 2006). Furthermore, EFs from previous studies may no longer be relevant due to improvements in emissions control technologies, removal of high-emitting vehicles, fleet-turnover, and changes in regulations. Significant multidecadal decreases in vehicle emissions of CO, VOC, NO_x, PM2.5 and BC have been observed previously (Jiang et al., 2005;McDonald et al., 2012;McDonald et al., 2013;Ban-Weiss et al., 2008;Bishop and Stedman, 2008;Dallmann et al., 2013).

Thus, the low fleet-average EFs obtained in this study indicate that the GTA fleet is clean relative to some of those listed for comparison in Table 2. In 1999, the government of Ontario introduced a vehicle testing program ("Drive Clean") aimed at improving air quality by identifying and removing/repairing high-emitting vehicles and resulting in a considerable decrease in smog-causing pollutants (NO_x and total hydrocarbons) of about 16% from program inception to 2010 (McCarter, 2012). Coincident with changes in gasoline regulations for benzene and other technology improvements, Canada introduced a Canada-Wide Standard for Benzene in 2010. Since then, the transportation sector has led a dramatic reduction in national average ambient concentrations of benzene, particularly in urban locations (Canada-Wide Standard for Benzene 2010 Final Report , 2012). Our relatively low EFs are hence consistent with the successful implementation of these and other policies, such as reduction in fuel sulfur content.

The most recent emission factor measurements for comparison were made at a near-road location in Toronto in 2013/2014 (Wang et al., 2015). The mean and median EFs for the VOCs, NO_x, PN, and BC obtained here are in excellent agreement with those reported by Wang et al. (2015) (see Fig. 4 and Fig. S5). The approach for determining EFs presented here differs in a) its mobile nature, covering a wide geographical area and range of road-types and b) its short time period (i.e., limited number of captured plumes). However, the mobile nature of our study results in a higher likelihood of sampling exhaust from a larger spectrum of vehicle types (including HDDVs) under a greater range of real-world driving conditions. The good agreement between the two studies for a wide range of pollutants gives confidence that our methodology provides representative fleet-average emission factors despite a smaller sample size. In this way the current study compliments the stationary study (Wang et al., 2015), demonstrating that the EFs obtained at their fixed location are applicable across a large region.

3.3.1. Black carbon emission factors

1   We obtained plume-based median and mean black carbon emission factors of 24.9 mg kg$_{fuel}$-

2   ^{1} and 85.6 mg kg$_{fuel}^{-1}$ respectively (IQR: 10.3 – 76.4 mg kg$_{fuel}^{-1}$). BC emission factors obtained by

3   prior tunnel, near-road, and mobile studies are listed in Table S9 for comparison. Literature

4   emission factors for HD diesel vehicles range from 160 – 2400 mg kg$_{fuel}^{-1}$, one to two orders of

5   magnitude higher than the literature emission factors for LD gasoline vehicles, which range from

6   ~1 – 300 mg kg$_{fuel}^{-1}$. LDGV emission factors at the high end of this range are from older studies in

7   more polluted environments (Westerdahl et al., 2009). In many of the earlier studies, BC emission

8   factors were obtained using aethelometers with a 1 min time resolution, which may not have been

9   fast enough to accurately quantify BC emission factors. In the current study, the poor performance

10   of the time-based approach with respect to yielding BC EFs in agreement with the plume-based

11   approach may also indicate that high time-resolution measurements of BC and good plume

12   definition are required to accurately estimate BC EFs from mobile measurements. However, more

13   comparisons are needed to determine if and how calculated BC EFs depend upon the BC

14   measurement method.

15   As was observed for the other pollutants (benzene, NO$_x$, PN etc.), the BC emission factors

16   obtained in this study are on the lower end of the reported literature range. Two studies have made

17   recent measurements of the mixed vehicle fleet in Toronto. Wang et al. (2015) made BC EF

18   measurements from their near-road stationary site in downtown Toronto using a photoacoustic

19   soot photometer and report a mean EF of (35 – 55) mg kg$_{fuel}^{-1}$. Liggio et al. (2012) obtained BC EFs

20   from transect driving downwind, and perpendicular to, a major Toronto highway (mean HDDV

21   fraction ~3.3%). The authors report fleet-average median emission factors of 59.3 mg kg$_{fuel}^{-1}$ (IQR:

22   27.0 – 148.4 mg kg$_{fuel}^{-1}$) using a HS-LII instrument and 29.4 mg kg$_{fuel}^{-1}$ (IQR: 11.8 – 66.0 mg kg$_{fuel}^{-1}$)

23   using a single-particle soot photometer. The values from these two studies (Wang et al., 2015;Liggio

24   et al., 2012) lie between the median and mean obtained in the current study.

25   The lower values obtained in this study compared to Liggio et al. could be reflective of

26   overall changes in the vehicle fleet over the past 5 years leading to reductions in BC emissions,

27   consistent with observations at other locations (Ban-Weiss et al., 2008;Dallmann et al., 2012). The

28   discrepancy between our study and the other two Toronto studies could also be related to location:

29   their fixed/limited sites may not be representative of the full fleet across the GTA. Given the

30   difference in LDGV and HDDV BC EFs, the emission factor calculation will be quite sensitive to the

31   frequency at which each vehicle type is sampled, which will be location-dependent. This sensitivity

32   can be quite dramatic: a recent study (Dallmann et al., 2013) found that due to their higher

33   associated BC emissions, even a small fraction (<1%) of heavy duty trucks can significantly bias the

34   calculated LDGV emission factors (by over 40%). For a pollutant exhibiting wide inter- and intra-

35   vehicle variation in EFs, obtaining measurements that capture the full fleet make-up over a range of

36   driving conditions is critical. Although we did not record the number of HDDVs (expected fraction ~

37   4%), the mobile design and scope of our study helps to mitigate location-specific results. Overall,

38   we found that the top 4% of plumes had vehicle emissions greater than 320 mg kg$_{fuel}^{-1}$ which are

39   typical of heavy-duty vehicles.

40   **3.3.2. HNCO emission factors**

1   As previously mentioned, literature HNCO EFs have been obtained exclusively from a limited
2   number of dynamometer studies (on both gasoline and diesel vehicles) and so a comprehensive
3   understanding of the real-world magnitude and variability of HNCO EFs is lacking. Here we obtain
4   the first fleet-average EFs for HNCO. Table 3 compares the HNCO emission factors available in the
5   literature with the wintertime plume-based HNCO median EF obtained in this study (2.3 mg kg_{fuel}^{-1}).
6   Our time-based analysis (Fig. 3b) suggests that HNCO EFs are similar in the summer and winter
7   (with slightly higher EFs in the summer, contrary to the behaviour of benzene).

8   Only two previous dynamometer studies (Brady et al., 2014; Suarez-Bertoa and Astorga, 2016)
9   obtained HNCO emission factors from gasoline vehicles and the average EFs reported from those
10   studies differ by more than an order of magnitude. HCNO was measured by Acetate-TOF-CIMS and
11   Fourier Transform Infrared Spectroscopy (FTIR) in the former (Brady et al., 2014) and latter
12   (Suarze-Bertoa and Astorga, 2016) studies, respectively. The plume-based median EF obtained in
13   this study is about a factor of two higher than that obtained by the earlier study (fleet average of
14   0.91±0.58 mg kg_{fuel}^{-1} for 8 LDGV) (Brady et al., 2014), but significantly lower than that obtained
15   more recently (fleet average of 93 mg kg_{fuel}^{-1} for 3 LDGV, or 29 mg kg_{fuel}^{-1} if the anomalously high
16   LDGV is omitted) (Suarez-Bertoa and Astorga, 2016).

17   Interestingly, emission factors ranging from 0.21 – 3.96 mg kg_{fuel}^{-1} were recently obtained from
18   an engine dynamometer study on a single light duty diesel engine, in agreement with the results
19   from the current study (Wentzell et al., 2013). This may suggest that HNCO emissions from gasoline
20   and diesel vehicles are of similar magnitude. In contrast, HNCO emission factors for an off-road
21   diesel engine have been found to be an order of magnitude higher, and it has been suggested that
22   the magnitude and range of HNCO emissions, as well as their dependence on operating conditions,
23   could be different for this type of engine (larger, off-road diesel engine) (Link et al., 2016;Jathar et
24   al., 2017). Much of the early work on HNCO vehicle emissions was prompted by the finding that
25   selective-catalytic reduction (SCR) systems could constitute an important source of HNCO (Kröcher
26   et al., 2005;Heeb et al., 2012;Heeb et al., 2011), but the impact of SCR systems (or other control
27   technologies such as the diesel particulate filter, DPF, or diesel oxidation catalyst, DOC) is disputed
28   (Jathar et al., 2017).

29   In addition to a wide range of emission factors, the available literature revealed conflicting
30   information on the conditions leading to elevated HNCO emissions, as well as high inter-vehicle
31   variability. HNCO emissions have been observed to vary by as much as an order of magnitude
32   depending on the driving cycle, but the influence of hard acceleration and cold engine starting is
33   contested (Brady et al., 2014;Suarez-Bertoa and Astorga, 2016). Similarly, studies have
34   demonstrated opposite trends for idle vs active operating conditions (Link et al., 2016;Wentzell et
35   al., 2013). For all these reasons, a direct comparison of the EF obtained in this study to reported EFs
36   is challenging. The current study cannot reveal the mechanism of HNCO production from diesel or
37   gasoline vehicles, or its dependence on factors such as driving condition and the presence of
38   various after-treatment technologies. However, a key strength of our study is that it is based upon a
39   large number of vehicles operating on-road in real-world conditions, thus implicitly reflecting a
40   range of these factors. Therefore, we suggest that the IQR reported here (1.37 – 4.15 mg kg_{fuel}^{-1})

1 along with the overall distribution of measured HCNO EFs (Fig. 4c) provides the most realistic
2 constraint to date on the magnitude and variability of HNCO emissions.

3.3.3. HCN emission factors

4   As with HNCO, EFs for HCN have been obtained exclusively from a limited number of
5 dynamometer studies. Table 4 lists HCN emission factors obtained in this study along with those
6 obtained from prior dynamometer studies; here distance-based units (mg km^{-1}) are used for ease of
7 comparison. The seasonal dependence of HCN vehicle emissions has not been previously studied.
8 Interestingly, Fig. 3c shows that the HCN EFs obtained using the time-based approach exhibit a
9 strong seasonal dependence, with the median summertime EF almost a factor 5 higher than the
10 median wintertime EF. This behaviour is opposite that of benzene, which has higher wintertime EFs
11 by about a factor of 2 due to enhanced cold-start emissions and changes in gasoline composition
12 (Lough et al., 2005). Although the mechanisms for HCN and benzene formation are different (the
13 former involving chemistry on high temperature catalysts), the reasons for the higher HCN EFs in
14 the summer are not known.

15   Early studies on some of the first generation three-way catalysts yielded very high HCN
16 emission factors, typically under abnormal or malfunctioning operating conditions (Bradow and
17 Stump, 1977;Keirns and Holt, 1978;Cadle et al., 1979;Urban and Garbe, 1979, 1980). The magnitude
18 of the HCN emissions exhibited high car-to-car variability and a strong dependence on operating
19 conditions, as well as the presence and composition of the catalysts. An average LDGV HCN EF of
20 12.1 mg km^{-1} was estimated from a review (Harvey et al., 1983) of these early studies – over two
21 orders of magnitude greater than the EFs obtained here. However, those EF estimations were
22 obtained for all driving modes for both normal and abnormal operating conditions.

23   Given the significant improvements in catalyst and emissions reduction technologies since the
24 1970s and 1980s, the applicability of these early studies to current HCN emission is questionable.
25 Certainly, more recent studies (Karlsson, 2004;Baum et al., 2006;Becker et al., 1999;Moussa et al.,
26 2016) suggest that present-day HCN EFs are much lower with individual vehicle EFs ranging from 0
27 – 11.7 mg km^{-1} (see Table 4). However, these limited dynamometer studies also reveal a large inter-
28 vehicle variability in HCN EFs, with no clear pattern between emissions and vehicle characteristics
29 (e.g. age). The most recent study (Moussa et al., 2016) also showed that intra-vehicle EFs are highly
30 sensitive to fuel injection technology (e.g. gasoline direct injection, GDI vs. port-fuel injection, PFI),
31 after-treatment technology (presence and absence of a particulate filter), and operating conditions
32 (e.g., aggressiveness of driving cycle, hot vs. cold-starts).

33   The median winter HCN EF obtained in this study (using either the plume-based or time-based
34 approach) is over an order of magnitude lower than the average EF obtained by the most recent
35 dynamometer study (Moussa et al., 2016). The higher summer HCN EF obtained by the time-based
36 analysis is in better agreement, although it is still low. However, due to the aforementioned
37 variability in the dynamometer results, a direct comparison is not straightforward. As with HNCO,
38 our study provides the most comprehensive HCN emission factors available to date since the
39 mobile design allows us to obtain EFs for a large number of vehicles, thereby capturing the real-
40 world inter- and intra-vehicle variability of emissions. Similarly, the IQR (0.32 – 0.88 mg kg$_{fuel}$$^{-1}$) and

1 distribution of measured EFs (Fig. 4d) give new insight into the range of on-road HCN emission
2 factors.

3.4. Emission factor distributions: contributions from high-emitters

4   The spread in the EFs for all measured pollutants is wide, consistent with prior mobile studies
5 (Park et al., 2011;Hudda et al., 2013;Zavala et al., 2009). Such variability is expected given the
6 differences in speed, acceleration, grade, and inter-vehicle variability occurring on-road. As
7 illustrated by Fig. 4 and Fig. S5, the EFs are log normally distributed, with the degree of skewness
8 dependent on pollutant. Skewness in EF distributions is typically attributed to the presence of
9 'high-emitting' vehicles among the fleet, but may also arise from the range and transient nature of
10 driving conditions experienced in the real-world (e.g., hard acceleration). The distributions provide
11 insight into the strategy for emission reductions. From a policy perspective, pollutants exhibiting a
12 more normal distribution may be most effectively targeted by tightening fleet-wide regulations
13 while those exhibiting a more skewed distribution may be most effectively targeted, initially, by the
14 removal of high-emitters (Hudda et al., 2013).

15   Cumulative emission factor distributions for several pollutants are presented in Fig. 5. These
16 plots highlight the relative skewness of EFs for each pollutant by displaying the fraction of total
17 emissions as a function of the fraction of vehicles, sorted from largest to smallest EF. The
18 distributions are highly skewed for NO and PN, and exceptionally skewed for BC, as observed by
19 others (Jiang et al., 2005;Hudda et al., 2013;Liggio et al., 2012). This behaviour is expected given
20 that these pollutants are emitted in large quantities from diesel-powered vehicles, which represent
21 a small fraction of the fleet (Jiang et al., 2005;Ban-Weiss et al., 2008;Jimenez et al., 2000;Dallmann
22 et al., 2012;Liggio et al., 2012;Wang et al., 2015;Ban-Weiss et al., 2010;Dallmann et al., 2013;Tan et
23 al., 2014) and hence were encountered by CRUISER less often. For NO, it is also likely that an
24 unknown quantity of emitted NO is being converted to NO_2 before plume capture (hence the high
25 frequency of EFs in the lowest bin, < 0.15 g kg_{fuel}^{-1}), further exacerbating the skewness. For BC, the
26 top 25% worst emitters, likely all diesel vehicles, contribute to more than 80% of the total
27 emissions, while the top 5% contribute to almost 50%. At a near-road site in Toronto, the top 25%
28 worst emitters were found to contribute to 100% of the total BC emissions, with the top 5%
29 contributing > 60% (Wang et al., 2015). As more heavy-duty vehicles become equipped with
30 particulate filters and advanced NO_x abatement technologies (i.e., SCR systems) the overall EF
31 distributions for pollutants such as BC and NO may shift, but the skewness could actually increase
32 unless high-emitters, such as the older, legacy diesel vehicles, are specifically targeted (McDonald et
33 al., 2013).

34   The EF distributions for the VOCs were less skewed (Jiang et al., 2005;Hudda et al.,
35 2013;Wang et al., 2015). The benzene, HNCO, and HCN profiles in Fig. 5 are similar, with the top
36 25% worst emitters contributing to 55-60% of the total emissions and the top 5% contributing 20-
37 30%. The less skewed distributions for HNCO and HCN may indicate that their HDDV EFs are not
38 significantly higher than their corresponding LDGV EFs. The least skewed pollutant in this study is
39 NO_2 – the top 25% worst emitters only contribute to ~50% of total emissions and the top 5%
40 contribute to ~15%. As suggested above, post-tailpipe conversion of NO to NO_2 is likely occurring

1 prior to measurement. The cumulative emission factor distribution for NO_x (=NO + NO_2) more
2 closely resembles the distribution for VOCs and NO_2 than NO.

3 **3.5. Vehicle emission estimates for Canada**

4 Annual emissions for Ontario and Canada can be estimated using the fuel-based EFs and from
5 annual sales of gasoline and diesel. The assumption here is that the gasoline and diesel sales are
6 proportional to the number of gasoline- and diesel-powered vehicles on the road, and that the EFs
7 obtained from the mobile measurements reflect this distribution. A summary of total vehicle
8 emissions of NO_x, benzene, BC, HNCO, and HCN calculated using the median plume-based emission
9 factors are given in Table 5. Nationwide inventory estimates for NO_x (Air Pollutants Emissions
10 Inventory), benzene (Canada-Wide Standard for Benzene 2010 Final Report, 2012), and BC
11 emissions (Canada's Black Carbon Inventory: 2017 Edition, 2017) by the transportation sector are
12 also listed in Table 5 for comparison. For all three pollutants, the scaled up emissions were more
13 than a factor of 2 lower than the inventory estimates. Using the mean EFs rather than median
14 reduces this discrepancy. Our results suggest that the inventories may be overestimated but more
15 work is required to understand the reasons for the difference.

16 We estimate that on a national scale, 104 tonnes of HNCO and 24 tonnes of HCN are emitted
17 annually by on-road vehicles. These values are lower than the recent nationwide estimates of 250 –
18 770 tonnes HNCO for 2010 (Wentzell et al., 2013) and 703 tonnes HCN for 2012 (Moussa et al.,
19 2016), owing to the lower fleet-average EFs obtained in this study. These vehicle emissions can be
20 placed in the context of their respective biomass burning emissions. Total wildfire emissions of CO
21 during the 2015 wildfire season (May 31, 2015 – Nov 2, 2015) were calculated using FireWork-
22 GEM-MACH (Pavlovic et al., 2016). These total CO emissions were then scaled by literature
23 emission ratios (ER) expressed as mol of pollutant per mol of CO to estimate biomass burning
24 emissions (Table 5). Only a few studies have investigated HNCO ERs (Veres et al., 2010;Roberts et
25 al., 2011). Biomass burning emissions of HCN have been the subject of a greater number of studies,
26 but a recent review notes that the HCN/CO ER can be different for different fire types and that even
27 within single or similar fire types there is a high variability in HCN emissions (Akagi et al., 2011).

28 In 2015, HNCO emissions from forest fires were estimated at 5377 tonnes and 40 tonnes for
29 Canada and Ontario respectively. Although on a national scale the HNCO vehicle emissions are over
30 an order of magnitude lower than the biomass burning emissions, in urban areas the vehicle source
31 becomes relatively more significant. This is seen in the provincial comparison, where the greater
32 population density and lower frequency of forest fires in Ontario results in HNCO vehicle emissions
33 comparable in magnitude to biomass burning emissions. When secondary formation of HNCO from
34 precursors in vehicle exhaust is also taken into account (Link et al., 2016;Liggio et al., 2017b), the
35 significance of vehicle emissions as a source of HNCO will likely be further enhanced.

36 In 2015, the HCN emissions from forest fires were estimated at $(1.2-5.8) \times 10^4$ tonnes and
37 (87-431) tonnes for Canada and Ontario respectively. At the national scale, the biomass burning
38 emissions are about 3 orders of magnitude greater than the vehicle emissions. Even at the
39 provincial scale, the biomass burning emissions are about an order of magnitude greater than the
40 vehicle emissions. This result is consistent with the large BKG component to the ambient

1 measurements made in the study. If the summertime EF obtained using the time-based approach is
2 used (2.7 mg kg_{fuel}^{-1}) then the total vehicle emissions of HCN are estimated at 125 tonnes and 44
3 tonnes for Canada and Ontario respectively, still lower than previous estimates (Moussa et al.,
4 2016). Although biomass burning emissions continue to be the dominant source of HCN in this
5 estimation, the potential significance of vehicles as a source of HCN, especially in urban areas with
6 minimal BB influence, is non-negligible.

7 **4. Conclusions and Implications**

8   We deployed a mobile laboratory over a large metropolitan area, capturing exhaust emissions
9 from a large number of vehicles under a range of operating conditions and driving environments.
10 Plume-based and time-based algorithms were developed to estimate EFs from the on-road
11 measurements. The plume-based method avoids cumbersome cross-reference with recorded
12 vehicle plumes (i.e, as in 'vehicle chase' methods) and shows potential for obtaining real-world EFs
13 from limited-term mobile studies with minimal computational effort. The time-based method was
14 found to perform well for pollutants with less skewed EF distributions (i.e., not associated with high
15 HDDV emissions), and best for pollutants with minimal local sources (i.e., HNCO and HCN). Further
16 studies are required to fully validate the time-based method, but this approach could potentially be
17 used to calculate EFs from near-road sites with lower time-resolution datasets. Both methodologies
18 could thus be efficient ways of rapidly monitoring trends in emission factors, especially for
19 pollutants whose emissions are likely to be influenced by emerging technologies or policies. Hence,
20 this approach could be valuable for documenting accountability.

21   Based on good agreement of the plume-based EFs with reported literature EFs for common
22 traffic pollutants, and the more precise definition of vehicle exhaust for this methodology, the
23 plume-based EFs are considered to be superior to the time-based EFs. Due to the broad range of
24 vehicles and real-world conditions captured by the measurements, the plume-based algorithm
25 applied to mobile measurements provides a better average EF for use in scaling-up emissions or for
26 assessing general exposure than a limited number of dynamometer studies. We thereby obtain the
27 first, and most representative fleet-average emission factors for HNCO and HCN, and insight into
28 their real-world variability.

29   The plume-based EF obtained for black carbon in this study (median: 25 mg kg_{fuel}^{-1}, IQR: 10
30 – 76 mg kg_{fuel}^{-1}) is consistent with decreases in vehicular BC emissions over time (Ban-Weiss et al.,
31 2008;Dallmann et al., 2013). Despite this improvement, our work, like that of others, shows that a
32 small number of vehicles (predominantly HDDV) are responsible for a disproportionate amount of
33 the on-road BC emissions. As a result, BC concentrations, and hence exposure, are highest near
34 highways and major roadways, and efforts to target these emissions will likely have a strong impact
35 on local air quality. In North America, GDI vehicles are replacing PFI vehicles, which currently
36 dominate the light-duty fleet (Chan et al., 2014). GDI vehicles promise advantages such as lower
37 fuel consumption, but have been shown in recent studies to emit more BC than their PFI
38 counterparts (Saliba et al., 2017) – although introduction of gasoline particulate filters could
39 mitigate this effect (Chan et al., 2014;Saliba et al., 2017). Future decreases in diesel emission of BC
40 are also predicted (Dallmann et al., 2012) as the fleet turns over and more diesel trucks on the road
41 are equipped with diesel particulate filters. Therefore, it is critical that fleet emissions of BC are

monitored in the future, with careful attention to the relative contributions from heavy-duty vs light-duty vehicles. Since BC also impacts global climate change (Highwood and Kinnersley, 2006;Bond et al., 2013), mitigating vehicle emissions of BC has the dual benefit of meeting air pollution and climate targets (Bahadur et al., 2011;Bond et al., 2013).

Overall, our results indicate that a vehicle fleet dominated by light duty gasoline vehicles is a source of HNCO and HCN to the atmosphere, with plume-based median EFs under wintertime, 'real-world', driving conditions of 2.3 mg kg_{fuel}^{-1} (IQR: 1.4 – 4.2 mg kg_{fuel}^{-1}) and 0.52 mg kg_{fuel}^{-1} (IQR: 0.32 – 0.88 mg kg_{fuel}^{-1}) respectively. Given our poor understanding of how emerging emission control technologies (e.g., SCR systems, diesel oxidation catalysts) influence HNCO emissions, it is imperative that fleet emissions of HNCO are studied over time. The impact of vehicle emissions on secondary HNCO production in urban areas should also be investigated.

Our work demonstrates that HCN emission factors obtained in out-dated dynamometer studies for LDGVs equipped with first-generation three-way-catalysts under abnormal operating conditions (Harvey et al., 1983) are not applicable to the present day. However, they indicate that the most recent dynamometer studies (Moussa et al., 2016;Karlsson, 2004) may also overestimate real-world HCN emissions. Overall, the relatively small vehicle emission factor obtained in this study suggests that vehicles are not likely a significant source of HCN on a regional and larger scale. However, in view of the discrepancies between this study and others (Moussa et al., 2016), and the paucity of HCN measurements in urban locations, more work is required to establish the atmospheric significance of vehicle emissions of HCN at the neighbourhood and smaller scale. In particular, the extent and cause of variation in HCN concentrations and emission factors, which appear to vary widely in ambient measurements and dynamometer studies respectively, should be further constrained and understood. Future research should also seek to understand the reasons for the observed seasonal variation in HCN concentrations and emission factors.

Supplement
Supplementary material related to this article is available.

Acknowledgements

We thank the technical support staff and information management/information technology team of AQRD for assistance with equipment and data system installation, data management, and driving. We thank Amy Leithead for assistance with the PTR-TOF-MS and Junhua Zhang for providing the wildfire CO estimates from Firework-GEM-MACH. This program was supported by the Clean Air Regulatory Agenda (CARA).

Competing Interests
The authors declare that they have no conflict of interest.

References

Air Pollutants Emission Inventory: https://pollution-waste.canada.ca/air-emission-inventory, access: 18 April 2018.

Akagi, S. K., Yokelson, R. J., Wiedinmyer, C., Alvarado, M. J., Reid, J. S., Karl, T., Crounse, J. D., and Wennberg, P. O.: Emission factors for open and domestic biomass burning for use in atmospheric models, Atmos. Chem. Phys., 11, 4039-4072, 2011.

Ambrose, J. L., Haase, K., Russo, R. S., Zhou, Y., White, M. L., Frinak, E. K., Jordan, C., Mayne, H. R., Talbot, R., and Sive, B. C.: A comparison of GC-FID and PTR-MS toluene measurements in ambient air under conditions of enhanced monoterpene loading, Atmos. Meas. Tech., 3, 959-980, 2010.

Ambrose, J. L., Zhou, Y., Haase, K., Mayne, H. R., Talbot, R., and Sive, B. C.: A gas chromatographic instrument for measurement of hydrogen cyanide in the lower atmosphere, Atmos. Meas. Tech., 5, 1229-1240, 2012.

Araizaga, A. E., Mancilla, Y., and Mendoza, A.: Volatile organic compound emissions from light-duty vehicles in Monterrey, Mexico: a tunnel study, Int. J. Environ. Res., 7, 277-292, 2013.

Bahadur, R., Feng, Y., Russell, L. M., and Ramanathan, V.: Impact of California's air pollution laws on black carbon and their implications for direct radiative forcing, Atmos. Environ., 45, 1162-1167, 2011.

Ban-Weiss, G. A., McLaughlin, J. P., Harley, R. A., Lunden, M. M., Kirchstetter, T. W., Kean, A. J., Strawa, A. W., Stevenson, E. D., and Kendall, G. R.: Long-term changes in emissions of nitrogen oxides and particulate matter from on-road gasoline and diesel vehicles, Atmos. Environ., 42, 220-232, 2008.

Ban-Weiss, G. A., Lunden, M. M., Kirchstetter, T. W., and Harley, R. A.: Size-resolved particle number and volume emission factors for on-road gasoline and diesel motor vehicles, J. Aerosol Sci., 41, 5-12, 2010.

Barillo, D. J.: Diagnosis and treatment of cyanide toxicity, J. Burn Care Res., 30, 148-152, 2009.

Barth, M. C., Cochran, A. K., Fiddler, M. N., Roberts, J. M., and Bililign, S.: Numerical modeling of cloud chemistry effects on isocyanic acid (HNCO), J. Geophys. Res. Atmos., 118, 8688-8701, 2013.

Baum, M. M., Moss, J. A., Pastel, S. H., and Poskrebyshev, G. A.: Hydrogen cyanide exhaust emissions from in-use motor vehicles, Environ. Sci. Technol., 41, 857-862, 2006.

Becker, K. H., Lörzer, Kurtenbach, R., Wiesen, P., Jensen, T. E., and Wallington, T. J.: Nitrous oxide (N_2O) emissions from vehicles, Environ. Sci. Technol., 33, 4134-4139, 1999.

Beckerman, B., Jerrett, M., Brook, J. R., Verma, D. K., Arain, M. A., and Finkelstein, M. M.: Correlation of nitrogen dioxide with other traffic pollutants near a major expressway, Atmos. Environ., 42, 275-290, 2008.

Bishop, G. A., and Stedman, D. H.: A decade of on-road emissions measurements, Environ. Sci. Technol., 42, 1651-1656, 2008.

Bond, T. C., Doherty, S. J., Fahey, D. W., Forster, P. M., Berntsen, T., DeAngelo, B. J., Flanner, M. G., Ghan, S., Kärcher, B., Koch, D., Kinne, S., Kondo, Y., Quinn, P. K., Sarofim, M. C., Schultz, M. G., Schulz, M., Venkataraman, C., Zhang, H., Zhang, S., Bellouin, N., Guttikunda, S. K., Hopke, P. K., Jacobson, M. Z., Kaiser, J. W., Klimont, Z., Lohmann, U., Schwarz, J. P., Shindell, D., Storelvmo, T., Warren, S. G., and Zender, C. S.: Bounding the role of black carbon in the climate system: A scientific assessment, J. Geophys. Res. Atmos., 118, 5380-5552, 2013.

Borduas, N., Abbatt, J. P., and Murphy, J. G.: Gas phase oxidation of monoethanolamine (MEA) with OH radical and ozone: kinetics, products, and particles, Environ. Sci. Technol., 47, 6377-6383, 2013.

Borduas, N., da Silva, G., Murphy, J. G., and Abbatt, J. P.: Experimental and theoretical understanding of the gas phase oxidation of atmospheric amides with OH radicals: kinetics, products, and mechanisms, J. Phys. Chem. A, 119, 4298-4308, 2015.

Borduas, N., Place, B., Wentworth, G. R., Abbatt, J. P. D., and Murphy, J. G.: Solubility and reactivity of HNCO in water: Insights into HNCO's fate in the atmosphere, Atmos. Chem. Phys., 16, 703-714, 2016.

Bradow, R. L., and Stump, F. D.: Unregulated emissions from three-way catalyst cars, SAE Tech. Pap. Ser., 770369, doi:770310.774271/770369, 1977.

Brady, J. M., Crisp, T. A., Collier, S., Kuwayama, T., Forestieri, S. D., Perraud, V., Zhang, Q., Kleeman, M. J., Cappa, C. D., and Bertram, T. H.: Real-time emission factor measurements of isocyanic acid from light duty gasoline vehicles, Environ. Sci. Technol., 48, 11405-11412, 2014.

Brook, J. R., Burnett, R. T., Dann, T. F., Cakmak, S., Goldberg, M. S., Fan, X., and Wheeler, A. J.: Further interpretation of the acute effect of nitrogen dioxide observed in Canadian time-series studies, J. Expo. Sci. Environ. Epidemiol., 17, S36, doi:10.1038/sj.jes.7500626, 2007.

Bukowiecki, N., Dommen, J., Prévôt, A. S. H., Richter, R., Weingartner, E., and Baltensperger, U.: A mobile pollutant measurement laboratory—measuring gas phase and aerosol ambient concentrations with high spatial and temporal resolution, Atmos. Environ., 36, 5569-5579, 2002.

Cadle, S. H., Nebel, G. J., and Williams, R. L.: Measurements of unregulated emissions from General Motors' light-duty vehicles, SAE Tech. Pap. Ser., 790694, doi:790610.794271/790694, 1979.

Canadian Council of Ministers of the Environment (CCME): Canada-Wide Standard for Benzene: 2010 Final Report, CCME, Winnipeg, Canada, 12 pp., January 2012.

Canagaratna, M. R., Jayne, J. T., Ghertner, D. A., Herndon, S., Shi, Q., Jimenez, J. L., Silva, P. J., Williams, P., Lanni, T., Drewnick, F., Demerjian, K. L., Kolb, C. E., and Worsnop, D. R.: Chase studies of particulate emissions from in-use New York City vehicles, Aerosol Sci. Technol., 38, 555-573, 2004.

Chan, T. W., Brook, J. R., Smallwood, G. J., and Lu, G.: Time-resolved measurements of black carbon light absorption enhancement in urban and near-urban locations of southern Ontario, Canada, Atmos. Chem. Phys., 11, 10407-10432, 2011.

Chan, T. W., Meloche, E., Kubsh, J., and Brezny, R.: Black Carbon Emissions in Gasoline Exhaust and a Reduction Alternative with a Gasoline Particulate Filter, Environ. Sci. Technol., 48, 6027-6034, 2014.

Chandra, B. P., and Sinha, V.: Contribution of post-harvest agricultural paddy residue fires in the N.W. Indo-Gangetic Plain to ambient carcinogenic benzenoids, toxic isocyanic acid and carbon monoxide, Environ. Int., 88, 187-197, 2016.

Choi, M. Y., Hamins, A., Mulholland, G. W., and Kashiwagi, T.: Simultaneous optical measurement of soot volume fraction and temperature in premixed flames, Combust. Flame, 99, 174-186, 1994.

Coderre, A. R., Thomson, K. A., Snelling, D. R., and Johnson, M. R.: Spectrally resolved light absorption properties of cooled soot from a methane flame, Appl. Phys. B, 104, 175-188, 2011.

Coggon, M. M., Veres, P. R., Yuan, B., Koss, A., Warneke, C., Gilman, J. B., Lerner, B. M., Peischl, J., Aikin, K. C., Stockwell, C. E., Hatch, L. E., Ryerson, T. B., Roberts, J. M., Yokelson, R. J., de Gouw, J. A.: Emissions of nitrogen-containing organic compounds from the burning of herbaceous and arboraceous biomass: Fuel composition dependence and the variability of commonly used nitrile tracers, Geophys. Res. Lett., 43, 9903- 9912, 1016.

Crounse, J. D., DeCarlo, P. F., Blake, D. R., Emmons, L. K., Campos, T. L., Apel, E. C., Clarke, A. D., Weinheimer, A. J., McCabe, D. C., Yokelson, R. J., Jimenez, J. L., and Wennberg, P. O.: Biomass burning and urban air pollution over the Central Mexican Plateau, Atmos. Chem. Phys., 9, 4929-4944, 2009.

Dallmann, T. R., DeMartini, S. J., Kirchstetter, T. W., Herndon, S. C., Onasch, T. B., Wood, E. C., and Harley, R. A.: On-road measurement of gas and particle phase pollutant emission factors for individual heavy-duty diesel trucks, Environ. Sci. Technol., 46, 8511-8518, 2012.

Dallmann, T. R., Kirchstetter, T. W., DeMartini, S. J., and Harley, R. A.: Quantifying on-road emissions from gasoline-powered motor vehicles: Accounting for the presence of medium- and heavy-duty diesel trucks, Environ. Sci. Technol., 47, 13873-13881, 2013.

Dominici, F., Peng, R. D., Barr, C. D., and Bell, M. L.: Protecting human health from air pollution: Shifting from a single-pollutant to a multi-pollutant approach, Epidemiology, 21, 187-194, 2010.

Environment and Climate Change Canada (ECCC): Canada's Black Carbon Inventory: 2017 Edition, ECCC, Canada, 29 pp., 2017.

Franco, V., Kousoulidou, M., Muntean, M., Ntziachristos, L., Hausberger, S., and Dilara, P.: Road vehicle emission factors development: A review, Atmos. Environ., 70, 84-97, 2013.

Gentner, D. R., Worton, D. R., Isaacman, G., Davis, L. C., Dallmann, T. R., Wood, E. C., Herndon, S. C., Goldstein, A. H., and Harley, R. A.: Chemical composition of gas-phase organic carbon emissions from motor vehicles and implications for ozone production, Environ. Sci. Technol., 47, 11837-11848, 2013.

Grahame, T. J., Klemm, R., and Schlesinger, R. B.: Public health and components of particulate matter: The changing assessment of black carbon, J. Air Waste Manag. Assoc., 64, 620-660, 2014.

Harvey, C. A., Garbe, R. J., Baines, T. M., Somers, J. H., Hellman, K. H., and Carey, P. M.: A study of the impact of some unregulated motor vehicle emissions, SAE Tech. Pap. Ser., 830987, doi:830910.834271/830987, 1983.

Heeb, N. V., Zimmerli, Y., Czerwinski, J., Schmid, P., Zennegg, M., Haag, R., Seiler, C., Wichser, A., Ulrich, A., Honegger, P., Zeyer, K., Emmenegger, L., Mosimann, T., Kasper, M., and Mayer, A.: Reactive nitrogen compounds (RNCs) in exhaust of advanced PM–NO$_x$ abatement technologies for future diesel applications, Atmos. Environ., 45, 3203-3209, 2011.

Heeb, N. V., Haag, R., Seiler, C., Schmid, P., Zennegg, M., Wichser, A., Ulrich, A., Honegger, P., Zeyer, K., Emmenegger, L., Zimmerli, Y., Czerwinski, J., Kasper, M., and Mayer, A.: Effects of a combined Diesel particle filter-DeNOx system (DPN) on reactive nitrogen compounds emissions: a parameter study, Environ. Sci. Technol., 46, 13317-13325, 2012.

HEI Panel on the Health Effects of Traffic-Related Air Pollution: Traffic-related air pollution: A critical review of the literature on emissions, exposure, and health effects, HEI Special Report 17, Health Effects Institute, Boston, MA, 386 pp., 2010.

Highwood, E. J., and Kinnersley, R. P.: When smoke gets in our eyes: The multiple impacts of atmospheric black carbon on climate, air quality and health, Environ. Int., 32, 560-566, 2006.

Ho, K. F., Lee, S. C., Ho, W. K., Blake, D. R., Cheng, Y., Li, Y. S., Ho, S. S. H., Fung, K., Louie, P. K. K., and Park, D.: Vehicular emission of volatile organic compounds (VOCs) from a tunnel study in Hong Kong, Atmos. Chem. Phys., 9, 7491-7504, 2009.

Hudda, N., Fruin, S., Delfino, R. J., and Sioutas, C.: Efficient determination of vehicle emission factors by fuel use category using on-road measurements: downward trends on Los Angeles freight corridor I-710, Atmos. Chem. Phys., 13, 347-357, 2013.

Hwa, M.-Y., Hsieh, C.-C., Wu, T.-C., and Chang, L.-F. W.: Real-world vehicle emissions and VOCs profile in the Taipei tunnel located at Taiwan Taipei area, Atmos. Environ., 36, 1993-2002, 2002.

Janssen, N. A., Hoek, G., Simic-Lawson, M., Fischer, P., van Bree, L., ten Brink, H., Keuken, M., Atkinson, R. W., Anderson, H. R., Brunekreef, B., and Cassee, F. R.: Black carbon as an additional indicator of the adverse health effects of airborne particles compared with PM10 and PM2.5, Environ. Health Perspect., 119, 1691-1699, 2011.

Jathar, S. H., Heppding, C., Link, M. F., Farmer, D. K., Akherati, A., Kleeman, M. J., de Gouw, J. A., Veres, P. R., and Roberts, J. M.: Investigating diesel engines as an atmospheric source of isocyanic acid in urban areas, Atmos. Chem. Phys., 17, 8959-8970, 2017.

Jerrett, M., Finkelstein, M. M., Brook, J. R., Arain, M. A., Kanaroglou, P., Stieb, D. M., Gilbert, N. L., Verma, D., Finkelstein, N., and Chapman, K. R.: A cohort study of traffic-related air pollution and mortality in Toronto, Ontario, Canada, Environ. Health Perspect., 117, 772-777, 2009.

Jiang, M., Marr, L. C., Dunlea, E. J., Herndon, S. C., Jayne, J. T., Kolb, C. E., Knighton, W. B., Rogers, T. M., Zavala, M., Molina, L. T., and Molina, M. J.: Vehicle fleet emissions of black carbon, polycyclic aromatic hydrocarbons, and other pollutants measured by a mobile laboratory in Mexico City, Atmos. Chem. Phys., 5, 3377-3387, 2005.

Jimenez, J. L., McRae, G. J., Nelson, D. D., Zahniser, M. S., and Kolb, C. E.: Remote sensing of NO and NO_2 emissions from heavy-duty diesel trucks using tunable diode lasers, Environ. Sci. Technol., 34, 2380-2387, 2000.

Joe, P., Belair, S., Bernier, N. B., Bouchet, V., Brook, J. R., Brunet, D., Burrows, W., Charland, J. P., Dehghan, A., Driedger, N., Duhaime, C., Evans, G., Filion, A.-B., Frenette, R., Grandpré, J. d., Gultepe, I., Henderson, D., Herdt, A., Hilker, N., Huang, L., Hung, E., Isaac, G., Jeong, C.-H., Johnston, D., Klaassen, J., Leroyer, S., Lin, H., MacDonald, M., MacPhee, J., Mariani, Z., Munoz, T., Reid, J., Robichaud, A., Rochon, Y., Shairsingh, K., Sills, D., Spacek, L., Stroud, C., Su, Y., Taylor, N., Vanos, J., Voogt, J., Wang, J. M., Wiechers, T., Wren, S., Yang, H., and Yip, T.: The Environment Canada Pan and ParaPan American Science Showcase Project, Bull. Amer. Meteor. Soc., In Press, 2018.

Jordan, A., Haidacher, S., Hanel, G., Hartungen, E., Märk, L., Seehauser, H., Schottkowsky, R., Sulzer, P., and Märk, T. D.: A high resolution and high sensitivity proton-transfer-reaction time-of-flight mass spectrometer (PTR-TOF-MS), Int. J. Mass Spectrom., 286, 122-128, 2009.

Karlsson, H. L.: Ammonia, nitrous oxide and hydrogen cyanide emissions from five passenger vehicles, Sci. Total Environ., 334-335, 125-132, 2004.

Keirns, M. H., and Holt, E. L.: Hydrogen cyanide emissions from three-way catalyst prototypes under malfunctioning conditions, SAE Tech. Pap. Ser., 780201, 1978.

Knighton, W. B., Fortner, E. C., Midey, A. J., Viggiano, A. A., Herndon, S. C., Wood, E. C., and Kolb, C. E.: HCN detection with a proton transfer reaction mass spectrometer, Int. J. Mass Spectrom., 283, 112-121, 2009.

Knox, A., Evans, G. J., Brook, J. R., Yao, X., Jeong, C. H., Godri, K. J., Sabaliauskas, K., and Slowik, J. G.: Mass absorption cross-section of ambient black carbon aerosol in relation to chemical age, Aerosol Sci. Technol., 43, 522-532, 2009.

Krecl, P., Johansson, C., Targino, A. C., Ström, J., and Burman, L.: Trends in black carbon and size-resolved particle number concentrations and vehicle emission factors under real-world conditions, Atmos. Environ., 165, 155-168, 2017.

Kristensson, A., Johansson, C., Westerholm, R., Swietlicki, E., Gidhagen, L., Wideqvist, U., and Vesely, V.: Real-world traffic emission factors of gases and particles measured in a road tunnel in Stockholm, Sweden, Atmos. Environ., 38, 657-673, 2004.

Kröcher, O., Elsener, M., and Koebel, M.: An ammonia and isocyanic acid measuring method for soot containing exhaust gases, Anal. Chim. Acta, 537, 393-400, 2005.

Kumar, V., Chandra B. P., Sinha, V. : Large unexplained suite of chemically reactive compounds present in ambient air due to biomass fires, Sci. Rep., 8, 626, doi:10.1038/s41598-017-19139-3, 2018.

Larson, T., Gould, T., Riley, E. A., Austin, E., Fintzi, J., Sheppard, L., Yost, M., and Simpson, C.: Ambient air quality measurements from a continuously moving mobile platform: Estimation of area-wide, fuel-based, mobile source emission factors using absolute principal component scores, Atmos. Environ., 152, 201-211, 2017.

Le Breton, M., Bacak, A., Muller, J. B. A., O'Shea, S. J., Xiao, P., Ashfold, M. N. R., Cooke, M. C., Batt, R., Shallcross, D. E., Oram, D. E., Forster, G., Bauguitte, S. J. B., Palmer, P. I., Parrington, M., Lewis, A. C., Lee, J. D., and Percival, C. J.: Airborne hydrogen cyanide measurements using a chemical ionisation mass spectrometer for the plume identification of biomass burning forest fires, Atmos. Chem. Phys., 13, 9217-9232, 2013.

Levy, I., Mihele, C., Lu, G., Narayan, J., Hilker, N., and Brook, J. R.: Elucidating multipollutant exposure across a complex metropolitan area by systematic deployment of a mobile laboratory, Atmos. Chem. Phys., 14, 7173-7193, 2014.

Li, Q., Jacob, D. J., Bey, I., Yantosca, R. M., Zhao, Y., Kondo, Y., and Notholt, J.: Atmospheric hydrogen cyanide (HCN): Biomass burning source, ocean sink?, Geophys. Res. Lett., 27, 357-360, 2000.

Li, Q., Jacob, D. J., Yantosca, R. M., Heald, C. L., Singh, H. B., Koike, M., Zhao, Y., Sachse, G. W., and Streets, D. G.: A global three-dimensional model analysis of the atmospheric budgets of HCN and CH_3CN: Constraints from aircraft and ground measurements, J. Geophys. Res. Atmos., 108, 8827, 2003.

Li, Q., Palmer, P. I., Pumphrey, H. C., Bernath, P., and Mahieu, E.: What drives the observed variability of HCN in the troposphere and lower stratosphere?, Atmos. Chem. Phys., 9, 8531-8543, 2009.

Li, S.-M., Leithead, A., Moussa, S. G., Liggio, J., Moran, M. D., Wang, D., Hayden, K., Darlington, A., Gordon, M., Staebler, R., Makar, P. A., Stroud, C. A., McLaren, R., Liu, P. S. K., O'Brien, J., Mittermeier, R. L., Zhang, J., Marson, G., Cober, S. G., Wolde, M., and Wentzell, J. J. B.: Differences between measured and reported volatile organic compound emissions from oil sands facilities in Alberta, Canada, Proc. Natl. Acad. Sci. U. S. A., 114, E3756-E3765, 2017.

Liggio, J., Gordon, M., Smallwood, G., Li, S.-M., Stroud, C., Staebler, R., Lu, G., Lee, P., Taylor, B., and Brook, J. R.: Are emissions of black carbon from gasoline vehicles underestimated? Insights from near and on-road measurements, Environ. Sci. Technol., 46, 4819-4828, 2012.

Liggio, J., Moussa, S. G., Wentzell, J., Darlington, A., Liu, P., Leithead, A., Hayden, K., O'Brien, J., Mittermeier, R. L., Staebler, R., Wolde, M., and Li, S. M.: Understanding the primary emissions and secondary formation of gaseous organic acids in the oil sands region of Alberta, Canada, Atmos. Chem. Phys., 17, 8411-8427, 2017a.

Liggio, J., Stroud, C. A., Wentzell, J. J. B., Zhang, J., Sommers, J., Darlington, A., Liu, P. S. K., Moussa, S. G., Leithead, A., Hayden, K., Mittermeier, R. L., Staebler, R., Wolde, M., and Li, S. M.: Quantifying the primary emissions and photochemical formation of isocyanic acid downwind of oil sands operations, Environ. Sci. Technol., 51, 14462-14471, 2017b.

Link, M. F., Friedman, B., Fulgham, R., Brophy, P., Galang, A., Jathar, S. H., Veres, P., Roberts, J. M., and Farmer, D. K.: Photochemical processing of diesel fuel emissions as a large secondary source of isocyanic acid (HNCO), Geophys. Res. Lett., 43, 4033-4041, 2016.

Logue, B. A., Hinkens, D. M., Baskin, S. I., and Rockwood, G. A.: The analysis of cyanide and its breakdown products in biological samples, Crit. Rev. Anal. Chem., 40, 122-147, 2010.

Lough, G. C., Schauer, J. J., Lonneman, W. A., and Allen, M. K.: Summer and winter nonmethane hydrocarbon emissions from on-road motor vehicles in the Midwestern United States, J. Air Waste Manag. Assoc., 55, 629-646, 2005.

Matz, C. J., Stieb, D. M., Brion, O.: Urban-rural differences in daily time-activity patterns, occupational activity and housing characteristics, 14, 88, doi:10.1186/s12940-015-0075-7, 2015.

Mauderly, J. L., and Samet, J. M.: Is there evidence for synergy among air pollutants in causing health effects?, Environ. Health Perspect., 117, 1-6, 2009.

McCarter, J.: 2012 Annual Report, Offic of the Auditor General of Ontario, Ontario, Canada, 457 pp., 2012.

McDonald, B. C., Dallmann, T. R., Martin, E. W., and Harley, R. A.: Long-term trends in nitrogen oxide emissions from motor vehicles at national, state, and air basin scales, J. Geophys. Res.: Atmos., 117, D00V18, doi:10.1029/2012JD018304, 2012.

McDonald, B. C., Gentner, D. R., Goldstein, A. H., and Harley, R. A.: Long-Term Trends in Motor Vehicle Emissions in U.S. Urban Areas, Environ. Sci. Technol., 47, 10022-10031, 2013.

Moussa, S. G., Leithead, A., Li, S.-M., Chan, T. W., Wentzell, J. J. B., Stroud, C., Zhang, J., Lee, P., Lu, G., Brook, J. R., Hayden, K., Narayan, J., and Liggio, J.: Emissions of hydrogen cyanide from on-road gasoline and diesel vehicles, Atmos. Environ., 131, 185-195, 2016.

Natural Resources Canada's Office of Energy Efficiency: Canadian Vehicle Survey: 2009 Summary Report, Natural Resources Canada, Ottawa, Canada, 72 pp., 2011.

Park, S. S., Kozawa, K., Fruin, S., Mara, S., Hsu, Y. K., Jakober, C., Winer, A., and Herner, J.: Emission factors for high-emitting vehicles based on on-road measurements of individual vehicle exhaust with a mobile measurement platform, J. Air Waste Manag. Assoc., 61, 1046-1056, 2011.

Parrish, D. D.: Critical evaluation of US on-road vehicle emission inventories, Atmos. Environ., 40, 2288, 2006.

Pavlovic, R., Chen, J., Anderson, K., Moran, M. D., Beaulieu, P.-A., Davignon, D., and Cousineau, S.: The FireWork air quality forecast system with near-real-time biomass burning emissions: Recent developments and evaluation of performance for the 2015 North American wildfire season, J. Air Waste Manag. Assoc., 66, 819-841, 2016.

Petzold, A., Ogren, J. A., Fiebig, M., Laj, P., Li, S. M., Baltensperger, U., Holzer-Popp, T., Kinne, S., Pappalardo, G., Sugimoto, N., Wehrli, C., Wiedensohler, A., and Zhang, X. Y.: Recommendations for reporting "black carbon" measurements, Atmos. Chem. Phys., 13, 8365-8379, 2013.

Pope, C. A., and Dockery, D. W.: Health effects of fine particulate air pollution: Lines that connect, J. Air Waste Manag. Assoc., 56, 709-742, 2006.

Rinsland, C. P., Dufour, G., Boone, C. D., Bernath, P. F., Chiou, L., Coheur, P.-F., Turquety, S., and Clerbaux, C.: Satellite boreal measurements over Alaska and Canada during June-July 2004: Simultaneous measurements of upper tropospheric CO, C_2H_6, HCN, CH_3Cl, CH_4, C_2H_2, CH_3OH, HCOOH, OCS, and SF_6 mixing ratios, Glob. Biogeochem. Cycles, 21, GB3008, doi:3010.1029/2006gb002795, 2007.

Roberts, J. M., Veres, P. R., Cochran, A. K., Warneke, C., Burling, I. R., Yokelson, R. J., Lerner, B., Gilman, J. B., Kuster, W. C., Fall, R., and de Gouw, J.: Isocyanic acid in the atmosphere and its possible link to smoke-related health effects, Proc. Natl. Acad. Sci. U. S. A., 108, 8966-8971, 2011.

Roberts, J. M., Veres, P. R., VandenBoer, T. C., Warneke, C., Graus, M., Williams, E. J., Lefer, B., Brock, C. A., Bahreini, R., Öztürk, F., Middlebrook, A. M., Wagner, N. L., Dubé, W. P., and de Gouw, J. A.: New insights into

atmospheric sources and sinks of isocyanic acid, HNCO, from recent urban and regional observations, J. Geophys. Res. Atmos., 119, 1060-1072, 2014.

Saliba, G., Saleh, R., Zhao, Y., Presto, A. A., Lambe, A. T., Frodin, B., Sardar, S., Maldonado, H., Maddox, C., May, A. A., Drozd, G. T., Goldstein, A. H., Russell, L. M., Hagen, F., and Robinson, A. L.: Comparison of gasoline direct-injection (GDI) and port fuel injection (PFI) vehicle emissions: Emission certification standards, cold-start, secondary organic aerosol formation potential, and potential climate impacts, Environ. Sci. Technol., 51, 6542-6552, 2017.

Sarkar, C., Sinha, V., Kumar, V., Rupakheti, M., Panday, A., Mahata, K. S., Rupakheti, D., Kathayat, B., and Lawrence, M. G.: Overview of VOC emissions and chemistry from PTR-TOF-MS measurements during the SusKat-ABC campaign: high acetaldehyde, isoprene and isocyanic acid in wintertime air of the Kathmandu Valley, Atmos. Chem. Phys., 16, 3979-4003, 2016.

Shim, C., Wang, Y., Singh, H. B., Blake, D. R., and Guenther, A. B.: Source characteristics of oxygenated volatile organic compounds and hydrogen cyanide, J. Geophys. Res. Atmos., 112, D10305; doi:10310.11029/12006JD007543, 2007.

Snelling, D. R., Smallwood, G. J., Liu, F., Gülder, Ö. L., and Bachalo, W. D.: A calibration-independent laser-induced incandescence technique for soot measurement by detecting absolute light intensity, Appl. Opt., 44, 6773-6785, 2005.

Statistics Canada: http://www.statcan.gc.ca/tables-tableaux/sum-som/l01/cst01/trade14b-eng.htm, access: 18 April 2018.

Stirn, R., Baquet, T. G., Kanjarkar, S., Meier, W., Geigle, K. P., Grotheer, H. H., Wahl, C., and Aigner, M.: Comparison of particle size measurements with laser-induced incandescence, mass spectroscopy, and scanning mobility particle sizing in a laminar premixed ethylene/air flame, Combust. Sci. Technol., 181, 329-349, 2009.

Suarez-Bertoa, R., and Astorga, C.: Isocyanic acid and ammonia in vehicle emissions, Transp. Res. D, 49, 259-270, 2016.

Tan, Y., Lipsky, E. M., Saleh, R., Robinson, A. L., and Presto, A. A.: Characterizing the spatial variation of air pollutants and the contributions of high emitting vehicles in Pittsburgh, PA, Environ. Sci. Technol., 48, 14186-14194, 2014.

Urban, C. M., and Garbe, R. J.: Regulated and unregulated exhaust emissions from malfunctioning automobiles, SAE Tech. Pap. Ser., 790696, doi:790610.794271/790696, 1979.

Urban, C. M., and Garbe, R. J.: Exhaust emissions form malfunctioning three-way catalyst-equipped automobiles, SAE Tech. Pap. Ser., 800511, doi:800510.842712/800511, 1980.

U. S. Environmental Protection Agency (EPA): Toxicological review of hydrogen cyanide and cyanide salts, U.S. EPA, Washington, D.C., 153 pp., September 2010.

Veres, P., Roberts, J. M., Warneke, C., Welsh-Bon, D., Zahniser, M., Herndon, S., Fall, R., and de Gouw, J.: Development of negative-ion proton-transfer chemical-ionization mass spectrometry (NI-PT-CIMS) for the measurement of gas-phase organic acids in the atmosphere, Int. J. Mass Spectrom., 274, 48-55, 2008.

Veres, P., Roberts, J. M., Burling, I. R., Warneke, C., de Gouw, J., and Yokelson, R. J.: Measurements of gas-phase inorganic and organic acids from biomass fires by negative-ion proton-transfer chemical-ionization mass spectrometry, J. Geophys. Res. Atmos., 115, D23302, doi:23310.21029/22010jd014033, 2010.

Wang, J. M., Jeong, C. H., Zimmerman, N., Healy, R. M., Wang, D. K., Ke, F., and Evans, G. J.: Plume-based analysis of vehicle fleet air pollutant emissions and the contribution from high emitters, Atmos. Meas. Tech., 8, 3263-3275, 2015.

Wang, Y., Xing, Z., Zhao, S., Zheng, M., Mu, C., and Du, K.: Are emissions of black carbon from gasoline vehicles overestimated? Real-time, in situ measurement of black carbon emission factors, Sci. Total Environ., 547, 422-428, 2016.

Wang, Z., Nicholls, S. J., Rodriguez, E. R., Kummu, O., Hörkkö, S., Barnard, J., Reynolds, W. F., Topol, E. J., DiDonato, A. J., Hazen, S. L.: Protein carbamylation links inflammation, smoking,uremia and atherogenesis, Nat. Med., 13, 1176–1184, 2007.

Wentzell, J. J., Liggio, J., Li, S. M., Vlasenko, A., Staebler, R., Lu, G., Poitras, M. J., Chan, T., and Brook, J. R.: Measurements of gas phase acids in diesel exhaust: a relevant source of HNCO?, Environ. Sci. Technol., 47, 7663-7671, 2013.

Westerdahl, D., Wang, X., Pan, X., and Zhang, K. M.: Characterization of on-road vehicle emission factors and microenvironmental air quality in Beijing, China, Atmos. Environ., 43, 697-705, 2009.

Woodward-Massey, R., Taha, Y. M., Moussa, S. G., and Osthoff, H. D.: Comparison of negative-ion proton-transfer with iodide ion chemical ionization mass spectrometry for quantification of isocyanic acid in ambient air, Atmos. Environ., 98, 693-703, 2014.

Wu, J. S., Krishnan, S. S., and Faeth, G. M.: Refractive indices at visible wavelengths of soot emitted from buoyant turbulent diffusion flames, J. Heat Transfer, 119, 230-237, 1997.

Yli-Tuomi, T., Aarnio, P., Pirjola, L., Mäkelä, T., Hillamo, R., and Jantunen, M.: Emissions of fine particles, NOx, and CO from on-road vehicles in Finland, Atmos. Environ., 39, 6696-6706, 2005.

You, Y., Staebler, R. M., Moussa, S. G., Su, Y., Munoz, T., Stroud, C., Zhang, J., and Moran, M. D.: Long-path measurements of pollutants and micrometeorology over Highway 401 in Toronto, Atmos. Chem. Phys., 17, 14119-14143, 2017.

Young, P. J., Emmons, L. K., Roberts, J. M., Lamarque, J.-F., Wiedinmyer, C., Veres, P., and VandenBoer, T. C.: Isocyanic acid in a global chemistry transport model: Tropospheric distribution, budget, and identification of regions with potential health impacts, J. Geophys. Res. Atmos., 117, D10308, doi:10310.11029/12011jd017393, 2012.

Zavala, M., Herndon, S. C., Slott, R. S., Dunlea, E. J., Marr, L. C., Shorter, J. H., Zahniser, M., Knighton, W. B., Rogers, T. M., Kolb, C. E., Molina, L. T., and Molina, M. J.: Characterization of on-road vehicle emissions in the Mexico City Metropolitan Area using a mobile laboratory in chase and fleet average measurement modes during the MCMA-2003 field campaign, Atmos. Chem. Phys., 6, 5129-5142, 2006.

Zavala, M., Herndon, S. C., Wood, E. C., Jayne, J. T., Nelson, D. D., Trimborn, A. M., Dunlea, E., Knighton, W. B., Mendoza, A., Allen, D. T., Kolb, C. E., Molina, M. J., and Molina, L. T.: Comparison of emissions from on-road sources using a mobile laboratory under various driving and operational sampling modes, Atmos. Chem. Phys., 9, 1-14, 2009.

Zhao, R., Lee, A. K. Y., Wentzell, J. J. B., McDonald, A. M., Toom-Sauntry, D., Leaitch, W. R., Modini, R. L., Corrigan, A. L., Russell, L. M., Noone, K. J., Schroder, J. C., Bertram, A. K., Hawkins, L. N., Abbatt, J. P. D., and Liggio, J.: Cloud partitioning of isocyanic acid (HNCO) and evidence of secondary source of HNCO in ambient air, Geophys. Res. Lett., 41, 6962-6969, 2014.

Zhao, Y., Strong, K., Kondo, Y., Koike, M., Matsumi, Y., Irie, H., Rinsland, C. P., Jones, N. B., Suzuki, K., Nakajima, H., Nakane, H., and Murata, I.: Spectroscopic measurements of tropospheric CO, C2H6, C2H2 and HCN in northern Japan, J. Geophys. Res. Atmos., 107, 4343-, 2002.

Zimmerman, N., Wang, J. M., Jeong, C. H., Ramos, M., Hilker, N., Healy, R. M., Sabaliauskas, K., Wallace, J. S., and Evans, G. J.: Field measurements of gasoline direct injection emission factors: Spatial and seasonal variability, Environ. Sci. Technol., 50, 2035-2043, 2016.
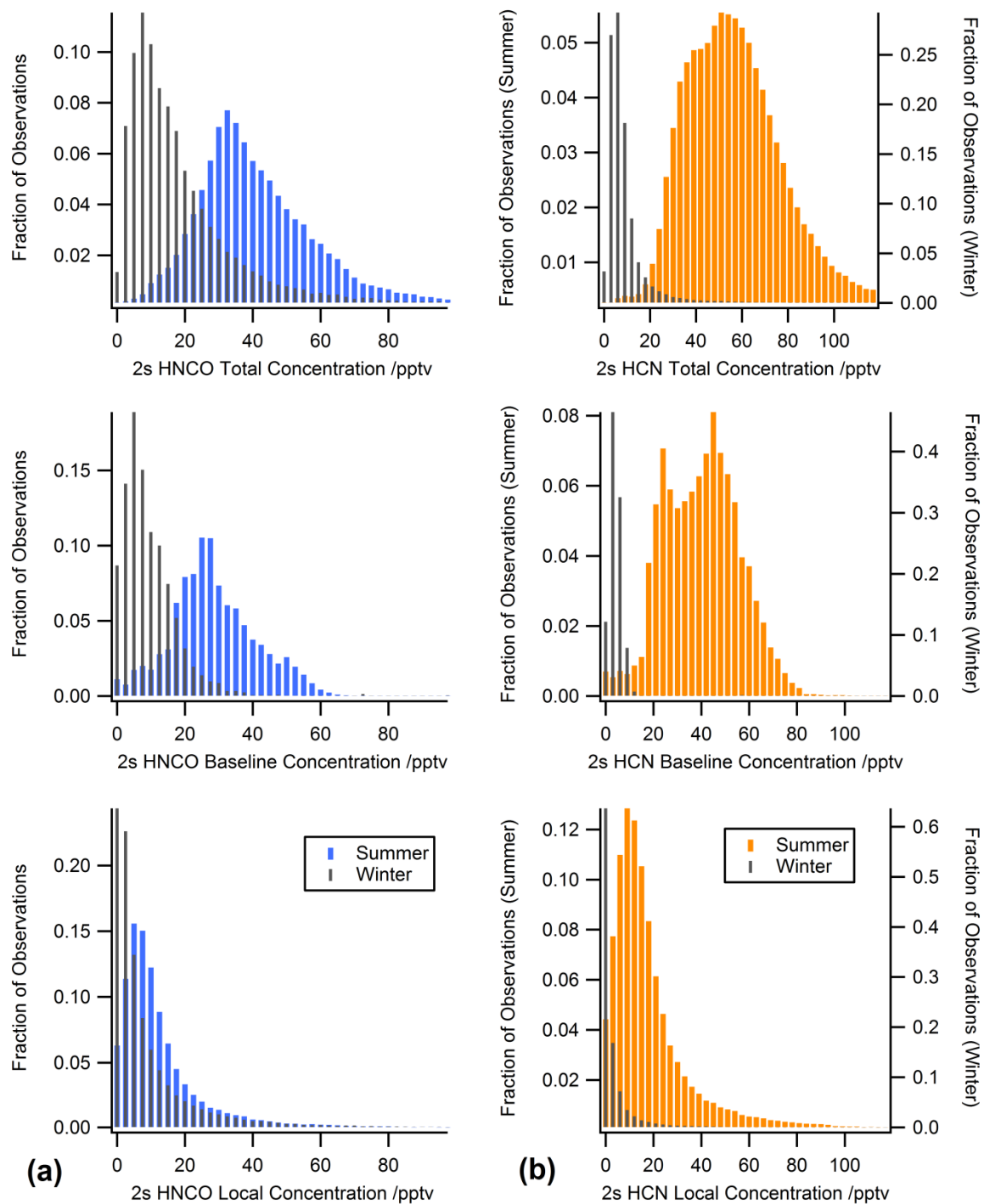
1   **Figures**

3   **Figure 1.** Distribution of ambient mixing ratios for (a) HNCO and (b) HCN. Top panel: total
4   concentration. Middle panel: background (BKG) concentration. Bottom panel: background-
5   corrected (LOCAL) concentration. Summer Campaign (July 2015) shown as colored bars, Winter
6   Campaign (Jan 2016) shown as grey bars.
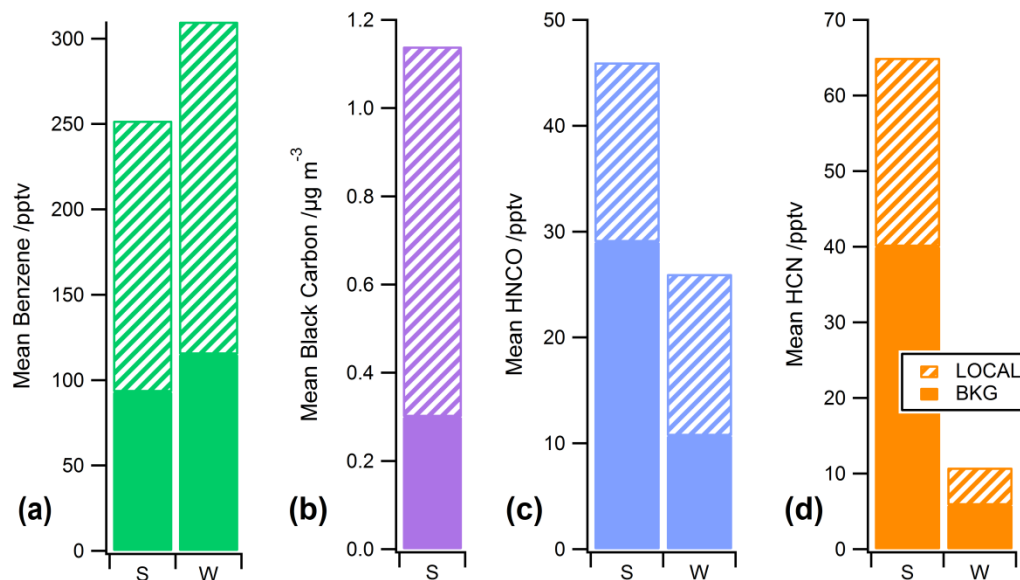
2 **Figure 2.** Mean on-road (LOCAL, patterned) and background (BKG, solid) mixing ratios for the
3 Summer (S) and Winter (W) Campaigns. (a) benzene, (b) BC, (c) HNCO, and (d) HCN.
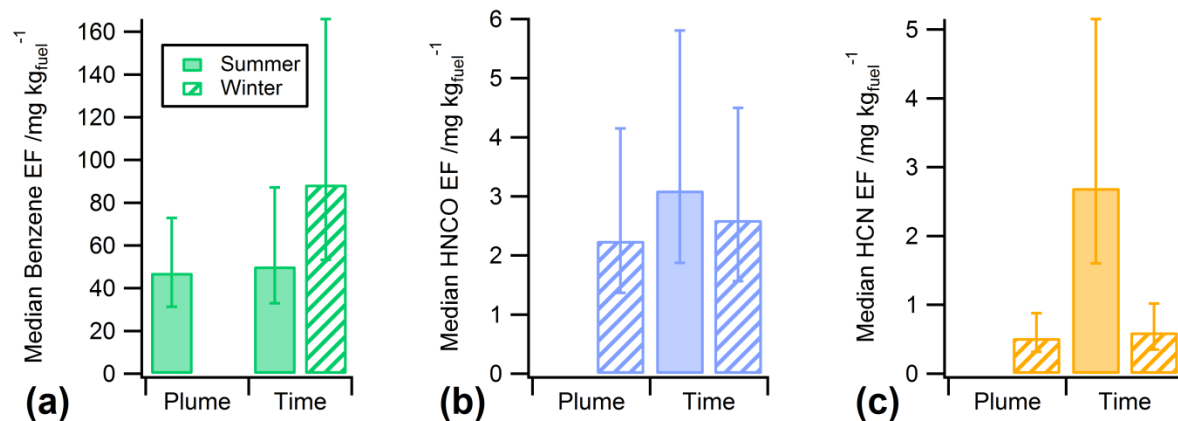
6 **Figure 3.** Median emission factors for (a) benzene, (b) HNCO, and (c) HCN calculated using the SPP
7 plume-based approach (Plume) or the time-based approach with an integration period of 120 s
8 (Time). The error bars show the interquartile range. Values obtained from the Summer Campaign
9 (solid bars) and Winter Campaign (patterned bars).
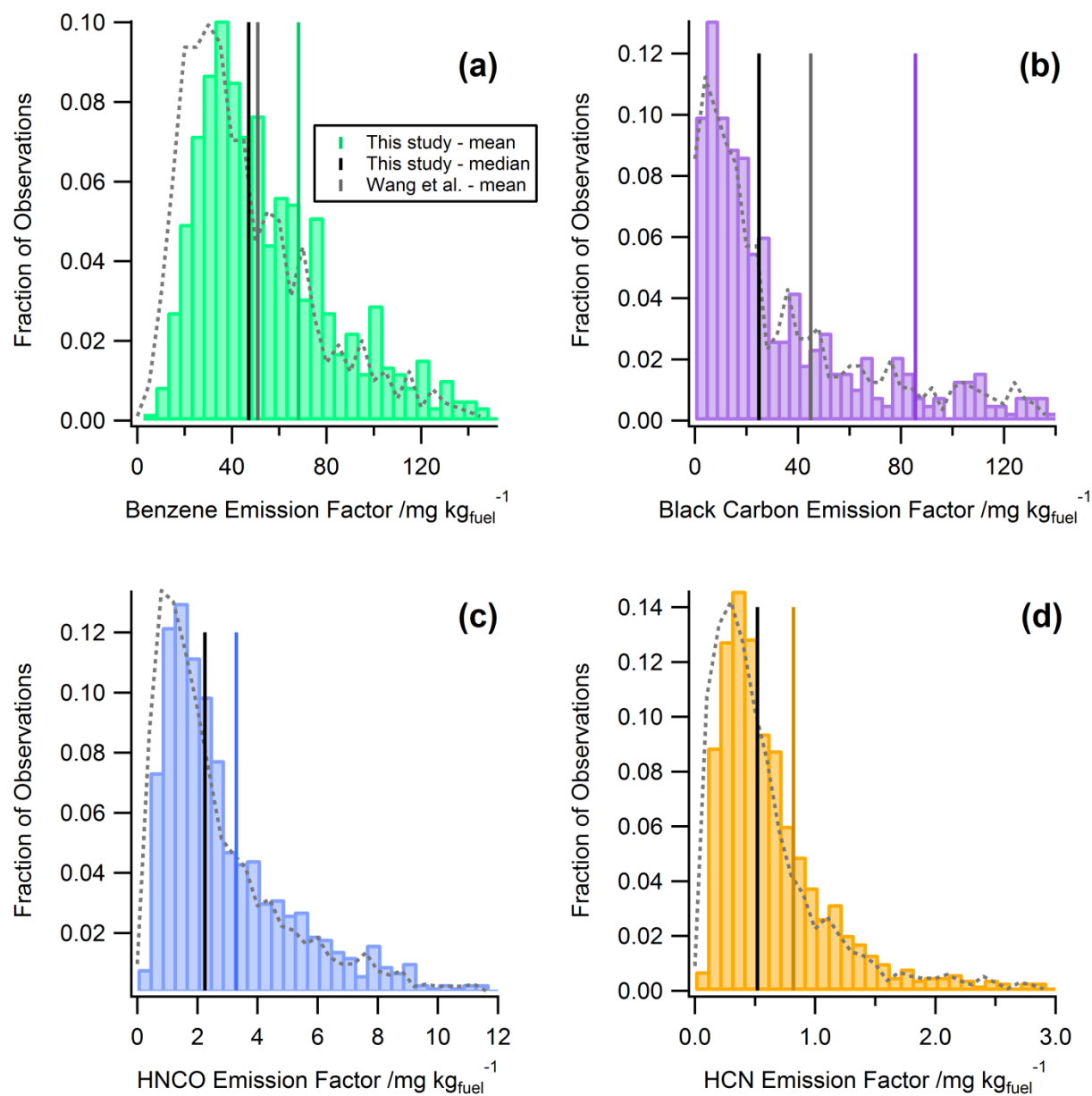
2 **Figure 4.** Plume-based emission factors obtained by CRUISER for (a) benzene, (b) BC, (c) HNCO,
3 and (d) HCN for the SPP case (colored bars) and the MPP case (grey, dashed line). The median and
4 mean EF values are indicated by the vertical black and colored lines respectively. Where available,
5 the mean EF obtained by Wang et al. (2015) is indicated by the vertical grey line.
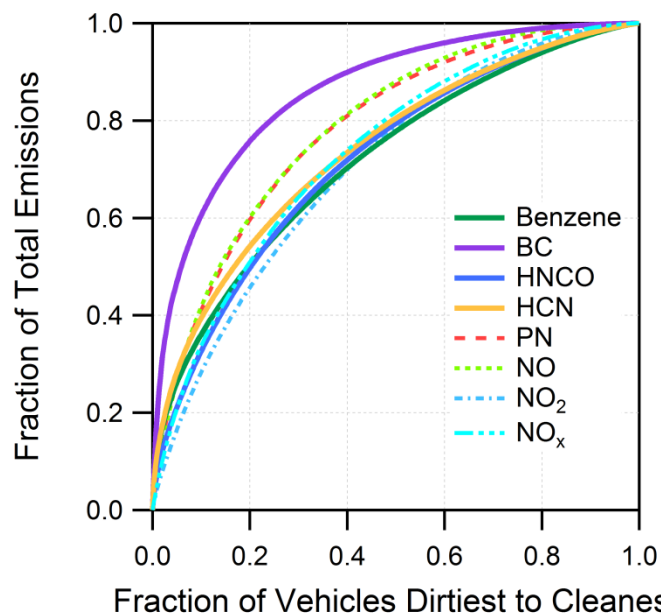
Figure 5. Cumulative emission factor distributions for SPP plume-based measurements: benzene
(solid, green), BC (solid, purple), HNCO (solid, blue), HCN (solid, yellow), NO (dotted, light green),
NO_2 (dotted, light blue), NO_x (dotted, light teal), particle number (dotted, pink). A 1 to 1 line would
indicate that all vehicles have the same emission factor.

3
4

1 **Tables**

2 **Table 1.** Method of detection and ambient concentration statistics for selected pollutants on
3 CRUISER

Pollutant and Units	Instrument	N	Mean (1σ)	Median	25th Percentile	75th Percentile	Max
Summer Campaign							
C6H6 /pptv	PTR-TOF-MS	112156	293 (1043)	170	91	320	170000
C7H8 /pptv	PTR-TOF-MS	113760	913 (3210)	382	198	757	395525
C8H10 /pptv	PTR-TOF-MS	112156	605 (224)	237	123	468	191205
NO$_2$ /ppbv	LGR[a]	99041	12.7 (13.3)	8.5	4.2	17.5	552
HNCO /pptv	HR-TOF-CIMS	103951	45.1 (39.0)	39.3	28.4	53.8	2168
HCN /pptv	HR-TOF-CIMS	103951	63.8 (52.4)	56.6	41.0	75.4	2429
NO /ppbv	TECO (42iTL)[b]	98036	20.9 (39.7)	6.2	2.0	21.2	998
CO$_2$ /ppmv	PICARRO[c]	59275	415 (33)	408	392	435	1893
PN[f] /1000# cm^{-3}	CPC[d]	98888	42.0 (87.4)	24.7	15.5	45.6	9230
Black Carbon /μg m^{-3}	HS-LII[e]	106075	1.06 (2.32)	0.38	0.16	0.97	43.4
Winter Campaign							
C6H6 /pptv	PTR-TOF-MS	131882	315 (294)	262	169	388	18500
HNCO /pptv	HR-TOF-CIMS	119642	25.7 (54.7)	15.5	8.8	27.1	2985
HCN /pptv	HR-TOF-CIMS	119642	10.6 (15.7)	7.7	5.4	11.2	1579
CO2 /ppmv	PICARRO[c]	78683	439 (30)	408	419	449	1250

Principles of Operation: [a]Cavity-enhanced laser absorption spectroscopy, [b]Thermo Scientific (42iTL) Chemiluminescence, [c]Cavity ring-down spectroscopy, [d]Light scattering, [e]Laser-induced incandescence. [f]PN=Ultrafine Particle Number Counts. Statistics obtained after self-sampling algorithm was applied to the high-time resolution data with N data points. All instruments operated at 1s resolution except PICARRO (2 s). The mean daily temperature was *ca.* 25 °C during the Summer Campaign and *ca.* -5 °C during the Winter Campaign.

1 **Table 2.** Plume-based median and mean emission factors calculated using single-peak plumes
2 (SPP) for the Summer and Winter Campaigns. Interquartile range (25th – 75th percentile) shown in
3 brackets. Units for numerator given in the pollutant column, units for denominator given in the
4 header.

Pollutant and Units	Fuel-based units $/kg_{fuel}^{-1}$	Distance-based units[a] $/km^{-1}$	Literature Range Fuel-based units[b] $/kg_{fuel}^{-1}$	References
SUMMER				
Benzene /*mg*	**47.2, 68.2** (31.3 - 72.8)	3.7, 5.7	**28 - 650**	Gentner et al., 2013; Hwa et al., 2002; Wang et al., 2015; Araizaga et al., 2013; Ho et al., 2009; Zavala et al., 2009; Kristensson et al., 2004
Toluene /*mg*	**101.6, 179.5** (62.5 - 194.6)	8.4, 14.9	**50 - 2075**	Hwa et al.,2002; Gentner et al., 2013; Wang et al., 2015; Araizaga et al., 2013; Ho et al. 2009; Zavala et al., 2009; Kristensson et al., 2004
C2 Benzenes[c] /*mg*	**76.8, 147.6** (44.8 - 149.7)	6.4, 12.2	**74 - 1455**	Hwa et al.,2002; Gentner et al., 2013; Wang et al., 2015; Araizaga et al., 2013; Ho et al. 2009; Zavala et al., 2009; Kristensson et al., 2004
NO$_2$[d] /*g*	**1.15, 1.39** (0.56 - 1.85)	0.095, 0.115		
NO[d] /*g*	**1.03, 1.79** (0.38 - 2.20)	0.086, 0.148		
NO$_x$ (=NO + NO$_2$) /*g*	**2.27, 3.13** (1.16 - 4.23)	0.188, 0.259	**1.4 - 42**	Wang et al., 2015; Kristensson et al., 2004; Hwa et al., 2002; Jiang et al., 2005; Hudda et al., 2013, Park et al., 2011; Dallmann et al., 2013; Kirchstetter et al., 1999; Ban-Weiss et al. 2008
Particle Counts /10^{14} #	**8.3, 15.9** (3.7 - 20.0)	0.69, 1.32	**3.9 - 57.4**	Wang et al., 2015; Kristensson et al., 2004; Hudda et al., 2013; Ban-Weiss et al., 2010
Black Carbon /*mg*	**24.9, 85.6** (10.3 - 76.4)	2.1, 7.1	**10 - 2400**	Literature Comparison in Table S9
WINTER				
HNCO /*mg*	**2.25, 3.30** (1.37 - 4.15)	0.126, 0.274	Literature Comparison in Table 5	
HCN /*mg*	**0.52, 0.82** (0.32 - 0.88)	0.043, 0.068	Literature Comparison in Table 6	

[a]Conversion from fuel-based units to distance-based units based on a fleet composed of 96% LDV with a fuel consumption rate of 10.6 L/100 km and 4% HDV (vehicles > 4.5 tonnes) with a fuel consumption rate of 28.5 L/100 km (based on the 2009 Canadian Vehicle Survey, and combining MDV with HDV) (Natural Resources Canada, 2012). Fuel densities at 15 °C of 730 kg m^{-3} (gasoline/LDV) and 840 kg m^{-3} (diesel/HDV) were used in all cases.

[b]For EFs reported in distance-based units, conversion to fuel-based units using stated distribution of gasoline and diesel vehicles and fuel consumption rates where available. When not stated, fuel consumption rates of 10.6 L/100 km for gasoline vehicles and 33.4 L/100 km for diesel vehicles were used (based on 2009 Canadian Vehicle Survey) (Natural Resources Canada, 2012). If the distribution of vehicles in the study was not stated or unclear the conversion was done assuming 96% gasoline and 4% diesel. Fuel densities at 15 °C of 730 kg m^{-3} (gasoline/LDV) and 840 kg m^{-3} (diesel/HDV) were used in all cases.

[c]C2 Benzenes corresponds to the sum of m-, p-, and o-xylene and ethylbenzene (protonated formula C8H11+). For literature reporting EFs for the individual species, the individual EFs were summed together.

[d]Comparison to literature made for NO$_x$ and not NO or NO$_2$ due to a) unknown conversion of NO to NO$_2$ post-tailpipe in our study and b) reporting of NO$_x$ rather than NO or NO$_2$ in the literature.

1   **Table 3.** Comparison of literature HNCO emission factors from the exhaust of various gasoline and
2   diesel fueled engines in fuel-based units (mg $\text{kg}_{\text{fuel}}^{-1}$).

Reference	Type of study	HNCO detection	Range /mg $\text{kg}_{\text{fuel}}^{-1}$	Average /mg $\text{kg}_{\text{fuel}}^{-1}$	Description of vehicle and fuel
This study	Mobile	HR-TOF-CIMS	1.4 – 4.2[a]	2.3, 3.3[b] 2.6, 4.0 3.1, 5.4	Winter fleet, plume-based (SPP) Winter fleet, time-based (120 s) Summer fleet, time-based (120 s)
Wentzell et al., 2013	Engine Dynamometer	Acetate-TOF-CIMS	0.21-3.96	NA	2011 Jetta equipped with turbo diesel injection (TDI) and diesel oxidation catalyst (DOC)
Brady et al., 2014	Chassis Dynamometer	Acetate-TOF-CIMS	0.45 – 1.70 (fleet averages for the 4 phases)	0.91±0.58 (full fleet, entire drive cycle)	8 LDGVs equipped with three way catalyst (TWC)
Suarez-Bertoa & Astorga, 2016	Chassis Dynamometer	FTIR	NA	30 (23 °C)[c] 140 (-7 °C)[c] 93 (23 °C)[d] 29 (23 °C)[e]	10 LDVs: 3 LDGV, 4 LDDV, 2 flex-fuel LDV, 1 electric LDV. Varying after-treatment
Heeb et al., 2011	Engine Dynamometer	Offline LC-MS analysis, after derivatization	NA	29 (with combined DPF-SCR system) 32 (with V_2O_5-based SCR system)	Diesel engine with a turbo charger and direct fuel engine, with and without selective catalytic reduction (SCR) and without diesel particulate filter (DPF)
Jathar et al., 2017	Engine Dynamometer	Acetate-TOF-CIMS	31 – 56	NA	John Deere PowerTech Plus (off-road) diesel engine with DOC and DPF, with and without SCR; diesel and biodiesel
Link et al., 2016	Engine Dynamometer	Acetate-TOF-CIMS	NA	54±3 (Idle) 17±2 (50% Load)	Same engine as above, with no DOC, DPF or SRC; diesel and biodiesel

[a]Interquartile range
[b]Median, Mean
[c]Fleet median for all 10 vehicles (all other values in the paper are reported in distance-based units mg km^{-1})
[d]Mean for the 3 gasoline vehicles (LDGVs)
[e]Mean for the gasoline vehicles omitting GV3 (anomalously high EFs)

1 **Table 4.** Comparison of literature HCN emission factors from the exhaust of various gasoline and
2 diesel fueled engines in distance-based units (mg km^{-1}).

Reference	Type of Study	HCN detection	Range /mg km^{-1}	Average /mg km^{-1}	Description of vehicles and fuel
This study	Mobile	HR-TOF-CIMS	0.03-0.07[a]	0.043, 0.068[b] 0.046, 0.069 0.21, 0.37	Winter fleet, plume-based (SPP) Winter fleet, time-based (120 s) Summer fleet, time-based (120 s)
Bradow and Stump, 1977	Chassis and Engine Dynamometer	Offline after trapping by NaOH	<LOD (normal operation) 0.0 – 75.6 (malfunctioning)	NA	3 LDGVs w/ TWC (1977) 5 LDGVs w/o TWC (1976)
Keirns and Holt, 1978	Chassis Dynamometer	Offline after trapping by NaOH	< 1.4 (LOD) (normal operation) 0.8 – 11.8 (malfunctioning)	NA	1 LDGV w/ and w/o TWC of varying composition (1977)
Cadle et al., 1979	Chassis Dynamometer	Trapping by NaOH with colorimetric detection	0-14.4	6.9 (no catalyst) 0.6 (oxidation catalyst) 3.1 (dual or three-way catalyst) 8.1 (rich malfunction with TWC)	26 LDGVs (production and experimental, 1967-1978)
Urban and Garbe, 1979	Chassis Dynamometer	Trapping by NaOH, GC-ECD	0.0 – 2.4 (normal) 0.3 - 2.3 (malfunctioning)	0.2 (normal, excluding LDV w/o catalyst)	5 LDGVs (1977-1978), 1 w/o catalyst, 4 w/ oxidation catalyst
Urban and Garbe, 1980	Chassis Dynamometer	Trapping by NaOH, GC-ECD	0.1 – 1.1 (normal) 0.0 – 112.3 (malfunctioning)		4 LDGVs with TWC (1978-1979)
Harvey et al., 1983	Review	NA	1.0 – 12.1 (weighted normal and malfunctioning averages for LDVs w/ different catalyst cases)	7.1	206 LDVs (non-catalyst, oxidation catalyst, TWC), 11 HDVs, gasoline and diesel
Becker et al., 1999	Chassis Dynamometer	FTIR	NA	< 2 (below LOD)	21 LDGVs (1996-1997)
Karlsson, 2004	Chassis Dynamometer	Trapping by NaOH with colorimetric detection	0.0 – 11.7	2.2 ±4.2	5 LDGVs (1989-1998)
Moussa et al., 2016	Chassis Dynamometer	PTR-TOF-MS	0.0 – 5.6	1.4±1.7	3 LDGV (2008-2011)

[a]Interquartile range
[b]Median, Mean

4

1 **Table 5.** Annual traffic pollutant emissions from the transportation sector and biomass burning for
2 Canada and Ontario

		NOx	Benzene	BC	HNCO	HCN
Canada 2015	Vehicle Emissions[a] (tonnes)	1.05×10^5	2180	1150	104	24
	Forest Fires[b] (tonnes)				5377[c]	$(1.2^d – 5.8^e) \times 10^4$
	Vehicle Emissions Inventory Estimates (tonnes)	4.26×10^{5f}	6600[g]	6401[h]		
Ontario 2015	Vehicle Emissions[a] (tonnes)	5.29×10^4	775	1410	37	9
	Forest Fires[b] (tonnes)				40[c]	87^d-431[e]

[a]In 2015, net sales for gasoline and diesel in Canada were 4.26×10^{10} L and 1.80×10^{10} L respectively (Statistics Canada). The total mass of fuel is calculated assuming a fuel density at 15 °C of 730 kg m^{-3} and 840 kg m^{-3} for gasoline and diesel respectively, for a nationwide total of 4.62×10^7 tonnes of fuel. In 2015, net sales of gasoline and diesel in Ontario were 1.63×10^{10} L and 5.43×10^9 L respectively, for a provincial total of 1.64×10^7 tonnes (Statistics Canada). Vehicle emissions calculated using the plume-based SPP emission factors.
[b]Wildfire CO emissions were calculated to be 5003 ktonnes and 37.3 ktonnes for Canada and Ontario, respectively
[c]HNCO emission calculated using HNCO/CO ER for Oak Woodland of 0.7 mmol HNCO mol CO^{-1} (Veres et al., 2010)
[d]HCN emission calculated using HNCO/CO ER of 0.00242 mol HCN mol CO^{-1} (Rinsland et al., 2007)
[e]HCN emission calculated using HNCO/CO ER of 0.012 mol HCN mol CO^{-1} (Akagi et al., 2011)
[f]Estimated NO$_x$ emissions for 2015 from light and heavy duty diesel and gasoline vehicles, trucks and motorcycles (Air Pollution Emission Inventory: https://pollution-waste.canada.ca/air-emission-inventory)
[g]Estimated on-road transportation benzene emissions for 2008 (Canada Wide Standard for Benzene: 2010 Final Report)
[h]Estimated BC emissions for 2015 from diesel (5679 tonnes) and gasoline (722 tonnes) on-road vehicles (Canada's Black Carbon Inventory: 2017 Edition)

5